

The Influence of Galaxy Formation Physics on Weak Lensing Tests of General Relativity

Andrew P. Hearin and Andrew R. Zentner

*Department of Physics and Astronomy, University of Pittsburgh,
Pittsburgh, PA 15260 USA*

E-mail: aph15+@pitt.edu, zentner+@pitt.edu

ABSTRACT: Forthcoming projects such as the Dark Energy Survey, Joint Dark Energy Mission, and the Large Synoptic Survey Telescope, aim to measure weak lensing shear correlations with unprecedented accuracy. Weak lensing observables are sensitive to both the distance-redshift relation and the growth of structure in the Universe. If the cause of accelerated cosmic expansion is dark energy within general relativity, both cosmic distances and structure growth are governed by the properties of dark energy. Consequently, one may use lensing to check for this consistency and test general relativity. After reviewing the phenomenology of such tests, we address a major challenge to such a program. The evolution of the baryonic component of the Universe is highly uncertain and can influence lensing observables, manifesting as modified structure growth for a fixed cosmic distance scale. Using two proposed methods, we show that one could be led to reject the null hypothesis of general relativity when it is the true theory if this uncertainty in baryonic processes is neglected. Recent simulations suggest that we can correct for baryonic effects using a parameterized model in which the halo mass-concentration relation is modified. The correction suffices to render biases small compared to statistical uncertainties. We study the ability of future weak lensing surveys to constrain the internal structures of halos and test the null hypothesis of general relativity simultaneously. Compared to alternative methods which null information from small-scales to mitigate sensitivity to baryonic physics, this internal calibration program should provide limits on deviations from general relativity that are several times more constraining. Specifically, we find that limits on general relativity in the case of internal calibration are degraded by only $\sim 30\%$ or less compared to the case of perfect knowledge of nonlinear structure.

KEYWORDS: dark energy theory, gravitational lensing, galaxy formation.

Contents

1. Introduction	1
2. Methods	4
2.1 Weak Lensing Observables	4
2.2 Parameterized Tests of the Consistency of General Relativity	7
2.3 Cosmological Parameters and Future Lensing Surveys	9
3. RESULTS	11
3.1 Consistency Checks	11
3.2 Biases	15
3.3 Calibration	20
4. Discussion	24
5. Summary	27

1. Introduction

Current data indicate that the cosmological expansion is accelerating (e.g., Refs. [1, 2, 3, 4, 5, 6, 7, 8, 9]). This accelerating expansion is one of the most profound discoveries of the past decade and points to a fundamental gap in our understanding of the universe. The cause of the accelerating expansion has been dubbed dark energy. Indeed dark energy is simply a name for the fundamental puzzle that is the nature of cosmic acceleration and an enormous amount of effort is now being devoted to shedding light on the causative agent of cosmic acceleration. In broadest terms, two options have been put forth to describe accelerated cosmic expansion. The first is that cosmic acceleration is caused by some as yet unidentified contribution to the stress energy of the universe. This option includes vacuum energy (observationally indistinguishable from a cosmological constant) and dynamical models of dark energy. The second option is that gravity deviates from the general relativistic description on large scales, an option we refer to as modified gravity.

Viable options to general relativity for which definite predictions have been made are few and far between, so many authors have suggested that a fruitful way to apply forthcoming data will be to check for the mutual consistency of different observable phenomena with the predictions of general relativity [10, 11, 12, 13, 14, 15, 16, 17].

The basic idea is that one may obtain observational handles on both the distance-redshift relation and the growth rate of cosmic expansion. Within general relativity, both of these can be predicted from the same dark energy parameters, so it is possible to measure, for example, distance and then check for consistency with the growth of cosmic structure. Forthcoming weak gravitational lensing surveys will provide the most powerful means to probe the matter distribution in the universe directly and are an indispensable piece of any such consistency check [10, 14]. A significant literature already exists detailing the power of tomographic weak lensing to constrain dark energy parameters, including Refs. [18, 19, 20, 21, 22, 23, 24, 25, 26, 27, 28, 29, 30, 31]. In fact, the effectiveness of any given matter fluctuation to serve as a lens is sensitive to the distance scale of the universe and so weak gravitational lensing alone will provide a very powerful check for the consistency of general relativity. In this manuscript, we study the effectiveness of such a consistency check in light of recent studies that indicate that predictions for weak lensing observables will contain significant inherent uncertainties due to the poorly-understood behavior of the baryonic component of the universe [32, 33, 34, 35, 31].

The strategy for checking the consistency of general relativity and searching for a sign of modified gravity outlined in the previous paragraph seems simple enough. However, making predictions for weak lensing power spectra is fraught with numerous practical difficulties. Weak lensing will use information on scales where density fluctuations are well beyond the linear regime (relative overdensities $\delta \gtrsim 1$). To utilize this information at the level that forthcoming observational programs will permit, numerical simulations must be able to predict the nonlinear matter power spectra to better than a percent [36, 37]. Sufficient precision should be achievable by brute force using dissipationless, N -body numerical simulations that treat only the evolution of the cosmic density field under gravity only (e.g., Refs. [38, 39, 40, 41]). The most challenging obstacle to such precise predictions is the significant influence that baryonic processes have on matter power spectra on scales of interest. This has been pointed out in both analytic [32, 33] and numerical studies [34, 35].

The problem posed by baryonic processes is severe because they cannot be modeled directly and all such calculations rely on relatively poorly-constrained, effective models that approximate the net, large-scale, effects of processes that occur on scales far below the numerical resolution that may be achieved with any simulation. Ref. [35] shows that the influences of baryons may be large compared with the statistical uncertainties expected of future surveys and that different treatments of baryonic physics lead to notably different matter power spectra on relevant scales. Ref. [31] studied a parameterized model for baryonic influences that could treat all of the simulations of Ref. [35] and showed that such a parameterized model could be calibrated self-consistently using weak lensing data alone, yielding meaningful constraints on both the dark energy and the effective models of baryonic physics. However, extending the results of Ref. [31] to consistency checks of general relativity

requires care. Baryonic processes manifest as an inability to predict the evolution of the density field even for a fixed cosmic expansion history. This is, in part, what Ref. [31] relied upon in their self-calibration program and this is precisely what proposed tests of the consistency of general relativity rely upon.

The strategy behind all efforts to study dark energy using gravitational lensing relies on the ability to produce reliable N -body simulations. In fact, most studies implicitly assume such a simulation campaign will be performed prior to any data analysis and proceed to estimate the power of forthcoming experiments using contemporary fitting formulae. In fact these fitting formulae are not sufficiently precise to treat forthcoming data, they may be subject to fundamental limitations [42, 43, 44, 40, 41], and, aside from a handful of specific cases, they have not been generalized to treat dark energy. A numerical campaign will be necessary to address dark energy and addressing observables using dissipationless N -body simulations is a challenging, but tractable problem [39, 41]. The results of N -body simulation campaigns represent precise solutions to the idealized problem of computing the density or lensing fields in a variety of cosmologies absent baryonic physics. As with dark energy constraints, the strategy of self-calibrating the net influences of baryons is based on the assumption that such a set of simulations without baryons are available and that a simple set of prescribed corrections can be applied to the N -body results to describe baryonic effects. The reason is that direct numerical calculations that treat the physics of baryons are not achievable in the foreseeable future, given current computational limitations. This is the context of the present paper.

In this paper, we extend the results of Ref. [31] to address consistency checks of general relativity. We present a brief pedagogical discussion of the manner in which independent modifications to the distance scale of the universe and the growth rate of structure produce non-degenerate changes in weak lensing statistics, enabling weak lensing alone to serve as a powerful consistency check for general relativity. We then move on to discuss the interplay between modifications to convergence spectra caused by baryonic processes and the dark energy. We show explicitly that our current ignorance regarding the evolution of the baryonic component of the universe, its influence on the evolution of inhomogeneities of dark matter, and the process of galaxy formation places a severe limitation on our ability to test the consistency of general relativity. To be specific, we consider two tests. In one test, the growth of structure and the cosmic distance scale are assumed to arise from two different effective equations of state w_g and w_d , and we test our ability to rule out the hypothesis that the two are equal as they would be in general relativity. If unaccounted for, our limited ability to predict convergence spectra can lead to biases that drive these two parameters to disagree at levels as large as $\sim 8\sigma$ (depending upon details) when general relativity is the correct description of gravity. We perform a similar test on the gravitational growth index parameter γ , introduced in Ref. [11], and likewise find significant biases if baryonic effects are not treated. We show that it is possible to

eliminate these biases by disregarding the small-scale shear information from forthcoming surveys, but the cost is a factor of $\sim 2 - 4$ degradation in the constraining power of such surveys. Lastly, we study the ability of forthcoming surveys to test general relativity and constrain baryonic processes simultaneously within a single data set. We show that this is a promising option as the biases can be eliminated at a cost of only $\sim 20\%$ in parameter constraints. This implies that significant effort should be devoted to developing robust parameterizations of the nonlinear evolution of structure as we begin to realize the next generation of imaging surveys. These methods should extend current techniques by including realistic descriptions of the effects of baryons that are not so general as to be completely arbitrary but do allow sufficient freedom so as to reflect our ignorance of the influence of the baryonic sector.

In the following section, we describe our methods, including our parameterizations of cosmological expansion and structure growth. In § 3, we present the results of our study. We begin in § 3.1 by illustrating the power of these consistency checks. This section contains a compilation of facts and figures found dispersed throughout the existing literature. In § 3.2, we show how neglect of baryonic processes may lead to biases that would mimic an inconsistency in general relativity in simpler treatments of weak lensing observables. In § 3.3, we present our results that show that additional parameter freedom may be added to predictions of the growth of structure to account for the influence of baryons and make such consistency checks robust to nonlinear processes. In § 4, we discuss our results and we summarize our efforts in § 5.

2. Methods

2.1 Weak Lensing Observables

We treat weak lensing observations as a consistency check of general relativity. Aside from our parameterization of dark energy, we perform all calculations as described in detail in Ref. [31]. We summarize those calculations here and refer the reader to this reference for more detail. We consider number density-weighted convergence power spectra and cross-spectra from $N_{\text{TOM}} = 5$ tomographic redshift bins as our primary observables:

$$P_{\kappa}^{\text{ij}}(\ell) = \int dz \frac{W_i(z)W_j(z)}{H(z)D_A^2(z)} P(k = \ell/D_A, z). \quad (2.1)$$

The five photometric redshift bins are spaced equally in redshift between a minimum photometric redshift of $z_p^{\text{min}} = 0$ and a maximum $z_p^{\text{max}} = 3$. Previous work showed that parameter constraints are saturated with $N_{\text{TOM}} = 5$ and that further binning is unnecessary [45, 31]. We have verified that this remains so in the models we consider. In Eq. (2.1), D_A is the angular diameter distance, $H(z)$ is the Hubble expansion rate, $P(k, z)$ is the matter power spectrum at wavenumber k and redshift z , and $W_i(z)$

are the lensing weight functions. Given the true redshift distribution of sources in bin i , dn_i/dz , the lensing weight is

$$W_i = \frac{3\Omega_M H_0^2}{2}(1+z)D_A \int \frac{D_A(z, z')}{D_A(z')} \frac{dn_i}{dz'} dz'. \quad (2.2)$$

We assume that the true redshift distribution of sources is

$$dn(z)/dz = 4\bar{n}(z/z_0)^2 \exp[-(z/z_0)^2]/\sqrt{2\pi z_0^2}, \quad (2.3)$$

where \bar{n} represents the total density of source galaxies per unit solid angle, which varies from survey to survey, and we assume $z_0 \simeq 0.92$ so that each survey has a median redshift of $z_{\text{med}} = 1$. We assume that the probability of a photometric redshift z_p given a spectroscopic redshift z is Gaussian with a mean value of z_p given by z (no bias) and a dispersion $\sigma_z = 0.05(1+z)$, and compute dn_i/dz for each photometric redshift bin as described in Ref. [45].

We estimate the constraining power of forthcoming weak lensing surveys using the Fisher information matrix. Indexing the observables of Eq. (2.1) by a single label, we write $\mathcal{O}_A = P_{\kappa}^{ij}$, where each i, j map onto a unique A , and the Fisher matrix of weak lensing observables is

$$F_{\alpha\beta} = \sum_{\ell_{\min}}^{\ell_{\max}} (2\ell + 1) f_{\text{sky}} \sum_{A,B} \frac{\partial \mathcal{O}_A}{\partial p_{\alpha}} [C^{-1}]_{AB} \frac{\partial \mathcal{O}_B}{\partial p_{\beta}} + F_{\alpha\beta}^{\text{P}}. \quad (2.4)$$

The p_{α} represent the parameters of the model, Greek indices label model parameters, capital Latin indices label unique observables, and lower-case Latin indices label tomographic redshift bins. f_{sky} is the fraction of sky covered by an experiment, C_{AB} is the covariance matrix of observables, and the sum begins at $\ell_{\min} = 2/\sqrt{f_{\text{sky}}}$ and runs to some ℓ_{\max} . We generally take $\ell_{\max} = 3000$ to ensure that we only use scales where assumptions of weak lensing and Gaussian statistics are valid [46, 47, 48, 49, 50]. However, we present many of our primary results (Figures 4, 5, 6, 7) as a function of ℓ_{\max} so results for alternative choices are simple to extract. Observed spectra contain both signal and noise, $\bar{P}_{\kappa}^{ij} = P_{\kappa}^{ij} + n_i \delta_{ij} \langle \gamma^2 \rangle$, where n_i is the surface density of source galaxies in bin i and $\langle \gamma^2 \rangle$ is the intrinsic source galaxy shape noise. We follow convention in setting $\langle \gamma^2 \rangle = 0.2$ and allowing differences in shape noise between different observations to be absorbed into n_i . The covariance between observables \bar{P}_{κ}^{ij} and \bar{P}_{κ}^{kl} is $C_{AB} = \bar{P}_{\kappa}^{ik} \bar{P}_{\kappa}^{jl} + \bar{P}_{\kappa}^{il} \bar{P}_{\kappa}^{jk}$, where i and j map to A , and k and l map to B .

The inverse of the Fisher matrix is an estimate of the parameter covariance near the maximum of the likelihood. The measurement error on parameter α marginalized over all other parameters is

$$\sigma(p_{\alpha}) = [F^{-1}]_{\alpha\alpha}. \quad (2.5)$$

The second term in Eq. (2.4) incorporates Gaussian priors on model parameters. We assume modest priors on several cosmological parameters individually, so that

$F_{\alpha\beta}^{\text{P}} = \delta_{\alpha\beta}/\sigma_{\alpha}^2$, where σ_{α} is the assumed prior uncertainty on parameter α . Unless otherwise stated, when we refer to the uncertainty in a parameter or subset of parameters, we are referring to the uncertainty in the parameters under discussion after marginalizing over the remaining parameters of the model. This formalism also provides an approximation for biases in cosmological parameter estimators due to unknown, untreated, systematic offsets in observables. Let $\Delta\mathcal{O}_{\text{A}}$ be the difference between the true observable and the prediction for that observable absent the systematic. The induced bias in the estimator of parameter α due to the neglect of the systematic offset is

$$\delta p_{\alpha} = \sum_{\beta} [F^{-1}]_{\alpha\beta} \sum_{\ell} (2\ell + 1) f_{\text{sky}} \sum_{\text{A,B}} \Delta\mathcal{O}_{\text{A}} [C^{-1}]_{\text{AB}} \frac{\partial \mathcal{O}_{\text{B}}}{\partial p_{\beta}}. \quad (2.6)$$

We model the matter power spectrum using the phenomenological halo model [51, 52, 53] (for a review see Ref. [54]). We use the particular implementation of Ref. [31]. This model utilizes standard fitting formulae for halo abundance and halo bias [55]. It is known that existing fitting formulae are not yet sufficiently precise to treat forthcoming data sets [42, 43], but it is likely that this can be overcome. Our approach is premised on the idea that dissipationless simulation programs will be carried out to calibrate these quantities to the necessary precision (or some equivalent strategy that utilized the simulation data directly), and that baryonic processes are the only processes that are not treated with sufficient precision. The non-standard modification to the halo model that we consider concerns the distribution of matter within dark matter halos. Typically, it is assumed that on average the mass density within a halo is described by the standard Navarro, Frenk, & White (NFW) density profile [56], $\rho \propto (cr/R_{200\text{m}})^{-1}(1 + cr/R_{200\text{m}})^{-2}$, where $R_{200\text{m}}$ is the halo virial radius which we define to contain a mean density of 200 times the mean density of the universe, the normalization is set by the fact that the mass profile must integrate to contain the total virial mass m within $R_{200\text{m}}$, and c is the halo concentration which sets the radius of the transition between the two power laws as $r_{\text{s}} \sim R_{200\text{m}}/c$.

The standard practice is to set the average concentration of a halo of mass m according to a phenomenological law derived from dissipationless N -body simulations, such as

$$c(m, z) = c_0 [m/m_{\star,0}]^{-\alpha} (1 + z)^{-\beta}, \quad (2.7)$$

where $c_0 \approx 10$, $\alpha \approx 0.1$, $\beta \approx 1$ [57, 58, 59], and $m_{\star,0}$ is the mass of a typical object collapsing at $z = 0$. We neglect the spread in halo concentrations at fixed mass because this gives rise to a negligible effect on the scales we consider, and on smaller scales this dispersion is degenerate with an overall shift in the concentration-mass relation [47, 60]. The shortcoming of Eq. (2.7) is that it describes halos in dissipationless N -body simulations that neglect the physics of baryons. Fortunately, Ref. [31] demonstrated that adopting a modified concentration-mass law within the

halo model suffices to model the convergence power spectra predicted by the baryonic simulations of Ref. [35] to a level where biases in inferred dark energy parameters are less than 10% of their statistical uncertainties for forthcoming surveys. We use this as a starting point for our preliminary estimate of the influence of baryonic processes on tests of the consistency of general relativity through weak gravitational lensing.

2.2 Parameterized Tests of the Consistency of General Relativity

As we mentioned in the introductory section, the ideal scenario would be to test parameterized families of theories for modified gravity that make specific and unique predictions; however, this is difficult at present. Few if any viable alternatives to general relativity that contain a contemporary epoch of accelerated expansion have been identified. Moreover, weak lensing requires some treatment of the evolution of density perturbations beyond the linear order of perturbation theory, and the nonlinear evolution of perturbations in models of modified gravity are not completely specified, nor have they been studied thoroughly. We consider two different parameterizations that have been proposed to test for the consistency of general relativity within forthcoming data. These do not represent complete, entirely self-consistent descriptions of any particular phenomenological alternative general relativity. We consider them as a pragmatic step toward testing the null hypothesis of gravity described by general relativity in the case of modest departures from the standard gravity. In both cases, we explore deviations to the linear growth of perturbations but assume that the relation between linear and nonlinear perturbations is unchanged. In practice, this means that we assume that halos of dark matter form with the abundances and other gross properties that they otherwise would have in a standard-gravity treatment and continue to employ the halo model to predict convergence spectra [Eq. (2.1)] on nonlinear scales ($\ell \gtrsim 300$). Modified gravity models require some environmental dependence to the gravitational force law so that gravity may deviate from general relativity on large scales (low density) yet satisfy local constraints on deviations from general relativity (in the high density environment of our galaxy) [61, 62, 63, 64, 65, 66, 67]. We do not consider any such modifications because there is no comprehensive treatment of the nonlinear evolution of perturbations in such theories and no phenomenological model akin to the halo model in the case of general relativity, though preliminary work in this direction has begun [67].

Our first test is to split the dark energy equation of state parameter into two distinct parameters. The first parameter, w_g , is used in all calculations of the growth of density perturbations while the second, w_d , is used in all calculations of the relationship between redshift and distance. The deflection of light is given by a sum of the Newtonian and curvature potentials and in the context of general relativity with zero anisotropic stress perturbation, these potentials are equal¹. This equality

¹We are admittedly a bit cavalier here as there are several different notational conventions in use,

means that perturbation growth and the distance-redshift relation are both determined by the evolution of the cosmic expansion rate $H(z)$, so that w_g and w_d should be equal in general relativity and that an indication to the contrary may be a sign of modified gravity. Of course, any observational or theoretical systematic errors that drive the inferred values of $w_g \neq w_d$ must be controlled and accounted for in order for this program to work. An alternative way to state our present aim is that we seek to assess the importance of the inability to predict the influence of the baryonic component of the universe on lensing power spectra for such consistency checks and explore a method to ensure the robustness of such a consistency check. In this first test, we consider our parameter set for dark energy to consist of the present dark energy density in units of the critical density Ω_{DE} , as well as the two equation of state parameters w_d and w_g . We take no priors on these parameters and set their fiducial values to $\Omega_{\text{DE}} = 0.76$, $w_d = w_g = -1$.

In the second case, we explore the gravitational growth index parameter γ , introduced by Linder in Ref. [11] and explored in Refs. [14, 15]. Linder showed that a natural separation between the expansion history of the universe and the growth of perturbations could be achieved by taking the evolution of an overdensity δ to be given by

$$\frac{d \ln \delta}{d \ln a} = \Omega_{\text{M}}(a)^\gamma. \quad (2.8)$$

Our notation is such that $a = 1/(1+z)$ is the cosmic scale factor, Ω_{M} with no argument of scale factor or redshift is the current density of non-relativistic matter in units of the critical density, $\Omega_{\text{M}}(a) = \Omega_{\text{M}} a^{-3} H_0^2 / H(a)^2$ with an explicit argument represents the evolution of the ratio of the matter density to the critical density, and $H_0 \equiv H(z=0) = 100h \text{ km/s/Mpc}$ is the present Hubble expansion rate. Eq. (2.8) holds for perturbations independent of scale or cosmic expansion history (aside from the dilution of $\Omega_{\text{M}}(a)$). In an enormous variety of dark energy models embedded within general relativity the growth index obeys [11, 14, 15]

$$\begin{aligned} \gamma &= 0.55 + 0.02[1 + w(z=1)], & \text{for } w < -1 \\ &= 0.55 + 0.05[1 + w(z=1)], & \text{for } w > -1, \end{aligned} \quad (2.9)$$

where $w(z)$ is the dark energy equation of state evaluated at redshift z . Deviations from this relation therefore, may indicate non-standard gravity. This treatment is accurate to better than a percent in specific cases such as the self-accelerating braneworld gravity model of Ref. [73] (so-called DGP gravity, which is now ruled

see Refs. [68, 69, 70, 71, 66, 72]; however, our contribution is not to explore the detailed behavior of the metric potentials in any specific theory (largely for lack of such options), so we forego a detailed discussion. In fact, we have already assumed the equality of the Newtonian and curvature potentials in order to derive Eq. (2.1) for the convergence power spectrum in terms of the power spectrum of density fluctuations and which would otherwise be written in terms of the power spectra of the metric potentials directly.

out as an explanation of the cosmic acceleration, see Ref. [74], but still serves as a useful example of the utility of this parameterization), which yields $\gamma \simeq 0.69$, as well as scalar-tensor and $f(R)$ theories of gravity [11, 15]. In this case, we consider the expansion history to be dictated by dark energy with abundance Ω_{DE} and a time-dependent effective equation of state $w(a) = w_0 + w_a(1 - a)$ [75], while perturbation growth is dictated by γ . We take no prior constraints on these parameters and perturb about the fiducial values $\Omega_{\text{DE}} = 0.76$ (as in the first case), $w_0 = -1$, $w_a = 0$, and $\gamma = 0.55$.

2.3 Cosmological Parameters and Future Lensing Surveys

In the previous section, we described the parameters we use to describe deviations from general relativistic gravity. To summarize, we take two test of the consistency of general relativity. In both cases, we assume dark energy with a present density of $\Omega_{\text{DE}} = 0.76$ in our fiducial model. In the first case, we split the dark energy equation of state parameter into two pieces, one governing the growth of density inhomogeneities w_g , and one governing the distance redshift relation w_d . We take as a fiducial model $w_g = w_d = -1$ and assume no priors on either parameter. In the second case, we assume dark energy with an effective equation of state $w(a) = w_0 + w_a(1 - a)$, with fiducial values $w_0 = -1$ and $w_a = 0$. In this case we assume inhomogeneity growth parameterized by γ according to Eq. (2.8), and take the fiducial value of $\gamma = 0.55$ as in general relativistic gravity with a cosmological constant causing contemporary acceleration.

Beyond the parameters that describe the dark energy/modified gravity sector, we consider four other cosmological parameters that influence lensing power spectra and may be degenerate with dark energy parameters. These parameters and their fiducial values are: the non-relativistic matter density $\omega_{\text{M}} \equiv \Omega_{\text{M}} h^2 = 0.13$, the baryon density $\omega_{\text{B}} = \Omega_{\text{B}} h^2 = 0.0223$, the amplitude of primordial curvature fluctuations $\Delta_{\mathcal{R}}^2 = 2.1 \times 10^{-9}$ (in practice we actually vary $\ln \Delta_{\mathcal{R}}^2$) at the pivot scale of $k_p = 0.05 \text{ Mpc}^{-1}$, and the power-law index of the spectrum of primordial density perturbations $n_s = 0.96$. We adopt conservative priors on each of these additional parameters that are comparable to contemporary constraints on each of these parameters individually [76]. To be specific, we take prior constraints of $\sigma(\omega_{\text{M}}) = 0.007$, $\sigma(\omega_{\text{B}}) = 10^{-3}$, $\sigma(\ln \Delta_{\mathcal{R}}^2) = 0.1$, and $\sigma(n_s) = 0.04$. Lastly, we allow three parameters that describe the effective concentrations of halos to be determined internally from the same data. These are the parameters $c_0 = 13$, $\alpha = 0.05$, and $\beta = 1$ of the power-law halo mass-concentration relation in Eq. (2.7). The fiducial values we choose, $c_0 \approx 10$ and $\alpha \approx 0.1$, differ from those found in N-body simulations of structure formation [discussion after Eq. (2.7)]. We choose these parameters to reflect the results of the hydrodynamic simulations of Ref. [35].

We study constraints that one would expect from three forthcoming galaxy imaging surveys. As mentioned in § 2.1, we follow current convention by setting the intrinsic

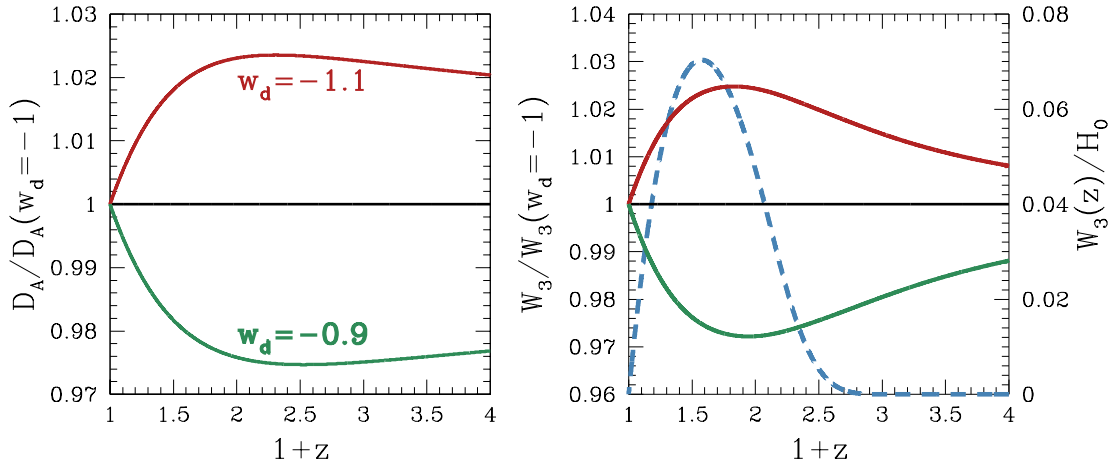


Figure 1: The influence of the dark energy equation of state parameter on the relationship between angular diameter distance and redshift. The *left* panel shows the angular diameter distance as a function of redshift for models with $w_d \neq -1$, in units of the angular diameter distance in our fiducial model with $w_d = -1$. The *upper* line shows D_A with $w_d = -1.1$ and the *lower* line shows D_A with $w_d = -0.9$. The *right* panel shows the net influence of this distance change on the lensing kernel of Eq. (2.2). The *dashed* line in this panel should be read against the right, vertical axis and represents the absolute weight $W_3(z)/H_0$. The solid lines show the particular example of the weight for the third tomographic bin $W_3(z)$ relative to its value in the $w_d = -1$ case and should be read against the left vertical axis. The correspondence with w_d is as in the *left* panel.

sic shape noise of source galaxies to be $\langle \gamma^2 \rangle = 0.2$ for all experiments and subsuming differences in the shape noise between surveys into differences in the effective number density of galaxies on the sky for each survey. We assume a redshift distribution of source galaxies as given in Eq. (2.3).

The most near-term survey that we explore is the dark energy survey (DES), which may begin operations in 2009 and have results as soon as 2011-2012². For the DES, we take $f_{\text{sky}} = 0.12$ and $\bar{n} = 15/\text{arcmin}^2$. We also consider an imaging survey that might be conducted as part of a future space-based mission such as the proposed Supernova Acceleration Probe (SNAP)³, which is a canonical example of a National Aeronautics and Space Administration, Beyond Einstein, Joint Dark Energy Mission probe⁴, though the specifics of the mission have yet to be decided and other competitors include the Advanced Dark Energy Physics Telescope (ADEPT)⁵ and the Dark Energy Space Telescope (DESTINY)⁶. For a SNAP-like probe, we

²<http://www.darkenergysurvey.org>

³<http://snap.lbl.gov>

⁴<http://universe.nasa.gov/program/probes/jdem>

⁵<http://universe.nasa.gov/program/probes/adept>

⁶<http://www.noao.edu/noao/staff/lauer/destiny>

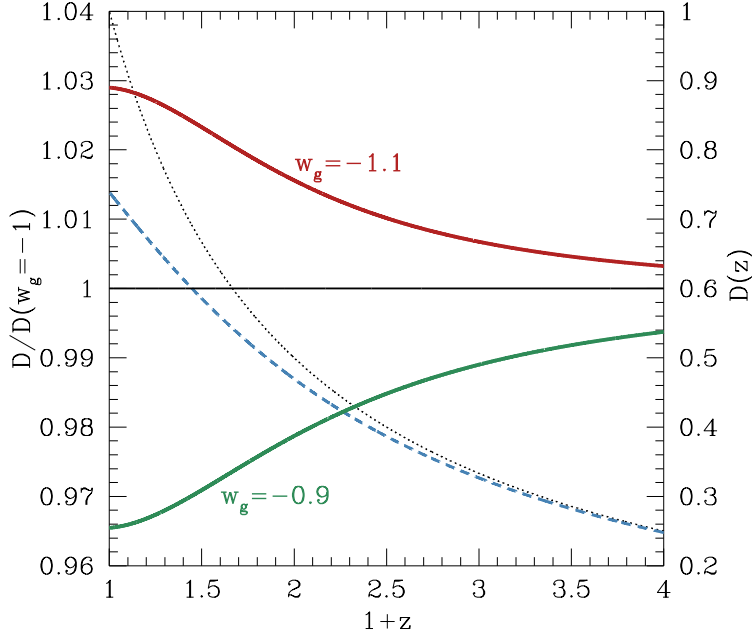


Figure 2: The influence of the dark energy equation of state parameter on the linear growth of structure over an observationally-relevant range of redshifts for forthcoming imaging surveys. We plot the linear growth function for dark energy with $w_g = -1.1$ (*upper line*) and $w_g = -0.9$ (*lower line*) as relative to the growth function in a cosmological constant model with $w_g = -1.0$. These relative shifts should be read against the left, vertical axis. In analogy with Fig. 1, we plot the absolute growth function for the standard case of $w_g = -1$ as the *dashed* line, which should be read against the right, vertical axis. The *dotted* line shows the growth function in a flat cosmological model with $\Omega_M = 1$ and $\Omega_{DE} = 0$ (and should again be read against the right, vertical axis). Comparing this growth rate to the growth rate in the fiducial model with $\Omega_{DE} = 0.76$ illustrates the suppression of growth caused by the contemporary epoch of accelerated expansion.

take $f_{\text{sky}} = 0.025$ and $\bar{n} = 100/\text{arcmin}^2$. Lastly, we consider a future ground-based imaging survey as might be carried out by the Large Synoptic Survey Telescope (LSST)⁷. We adopt $f_{\text{sky}} = 0.5$ and $\bar{n} = 50/\text{arcmin}^2$ to describe the LSST survey. In all cases we consider only the statistical limitations of the surveys. The only systematic uncertainty we consider is the theoretical uncertainty associated with the inability to make precise predictions of the net influence of baryons on the lensing power spectra.

3. RESULTS

3.1 Consistency Checks

We begin by illustrating the power of weak lensing surveys to test the consistency of

⁷<http://lsst.org>

general relativity with forthcoming data. As we have mentioned above, the consistency checks work by comparing simultaneous constraints on cosmological distances and structure growth and determining whether they are consistent with a single, underlying, general relativistic model. Before moving on to parameter constraints we briefly discuss each of these effects individually. We will use the split dark energy parameterization model (with parameters w_g and w_d) to illustrate the influence of modified distances and modified growth. Those readers with significant experience with dark energy phenomenology and proposed consistency checks of general relativity may like to proceed to the next section.

The influence of dark energy on the cosmic distance scale is demonstrated in Figure 1. The left panel of this figure shows the angular diameter distance as a function of redshift in dark energy models with constant equations of state $w_d = -1.1$, $w_d = -1.0$, and $w_d = -0.9$. The more negative the equation of state parameter, the more recent the prevalence of dark energy, and the more rapid is the current acceleration. Thus, for a fixed present Hubble expansion rate, lower values of w_d lead to larger angular diameter distances. The dependence of the angular diameter distance on the dark energy equation of state manifests in the lensing weight [Eq. (2.2)]; this dependence implies that the lensing weight varies with w_d . The effects of this dependence are shown in the right panel of Fig. 1 for the particular case of the weight for the third tomographic bin containing $W_3(z)$, which contains sources with photometric redshifts in the range $1.2 \leq z_p < 1.8$. Notice that the lens weight itself (dashed line) extends to $z > 1.8$. In our model, sources in this bin have true redshifts that extend beyond $z = 1.8$ because of the relatively large dispersion in calibrated photometric redshifts. For more negative w_d , the $W_3(z)$ is relatively increased and weighted relatively more toward low redshift. Heuristically, this can be understood by considering a hypothetical individual deflector. Relative to the deflector, the angle of deflection of a light ray is fixed by the deflector properties and the apparent change of position of the source as seen by an observer grows with angular diameter distance. The varying distances to fixed redshift also affect the mapping between multipole and wavenumber in the matter power spectrum at fixed redshift. Increased distances mean smaller wavenumber at fixed redshift, and as the power spectrum of density fluctuations is a declining function of wavenumber on scales of interest, this results in slightly stronger lensing.

Next, we demonstrate the dependence of the cosmic growth function on dark energy. Figure 2 shows the growth function $D(z)$ in our fiducial cosmology (dashed line), normalized such that $D(z) \rightarrow (1+z)^{-1}$ as $z \rightarrow \infty$. The dashed line in this figure shows the growth function in a flat cosmological model with no dark energy and $\Omega_M = 1$. Comparing these two growth functions shows the dramatic suppression in the growth of density perturbations during the epochs where dark energy makes a significant contribution to the cosmic energy budget. In addition, we show the growth functions in cosmological models with $w_g = -1.1$ and $w_g = -0.9$ relative to the

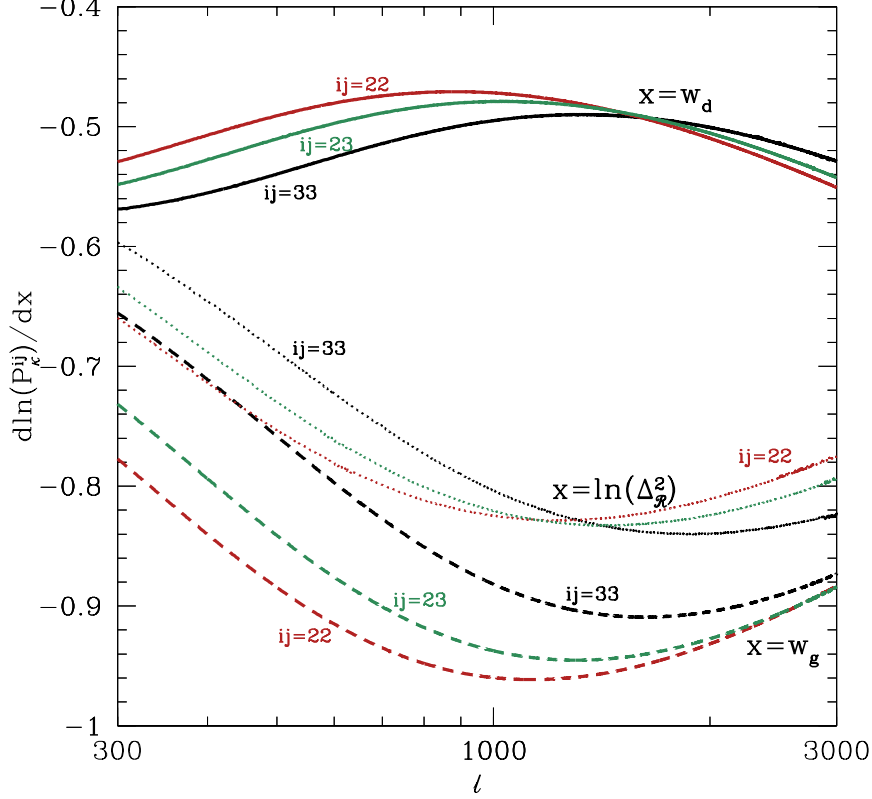


Figure 3: Partial derivatives of tomographic weak lensing power spectra with respect to cosmological parameters. We show derivatives of each of the power spectra $P_{\kappa}^{ij}(\ell)$, with $ij = 22, 23, 33$ with respect to the three parameters w_d , w_g , and $\ln \Delta_{\mathcal{R}}^2$. The *solid* lines show derivatives with respect to w_d . From bottom to top at left, the *solid* lines are $\partial \ln P_{\kappa}^{ij} / \partial w_d$ with $ij = 33, 23, 22$. The *dashed* lines represent derivative with respect to w_g . From bottom to top at left, the *dashed* lines show $\partial \ln P_{\kappa}^{ij} / \partial w_g$ with $ij = 22, 23, 33$. The *dotted* lines are derivatives with respect to the power spectrum normalization parameter $\ln \Delta_{\mathcal{R}}^2$. From bottom to top at left, the *dotted* lines show $-\partial \ln P_{\kappa}^{ij} / \partial \ln \Delta_{\mathcal{R}}^2$ with $ij = 22, 23, 33$. The additional negative sign for the derivatives with respect to $\ln \Delta_{\mathcal{R}}^2$ is designed to reduce the dynamic range on the vertical axis.

growth function in our fiducial model. The more positive the dark energy equation of state is, the earlier the acceleration begins and the earlier the growth of structure is quenched by the competing cosmic expansion. Conversely, more negative values of the dark energy equation of state lead to more recent expansion and, as a result, more aggregate growth of density perturbations since the epoch of recombination. These features are all represented in Fig. 2.

The modifications to the growth of structure and cosmic distances manifest as changes in the observable power spectra. Figure 3 shows partial derivatives of three

of the power spectra, P_{κ}^{22} , P_{κ}^{33} , and P_{κ}^{23} , as a function of parameters w_d , w_g , and $\ln \Delta_{\mathcal{R}}^2$. The derivatives with respect to the dark energy parameters are all negative. To reduce the range of the vertical axis, we actually display $-dP_{\kappa}^{ij}/d \ln \Delta_{\mathcal{R}}^2$, so that it will also lie in the negative vertical half plane. Notice that variations in the observable power spectra due to changes in w_g and w_d have very different redshift and scale dependence. Consequently, we should not expect these parameters to exhibit a significant degeneracy and we would expect that shear power spectrum observations could constrain both parameters independently. Notice also that changes in w_g induce relatively larger shifts in the observable power spectra than do shifts in w_d . In the absence of additional information, this might be taken as evidence that weak lensing constraints on w_g should be more stringent than such constraints on w_d . In practice, w_g is strongly degenerate with the power spectrum normalization parameter $\ln \Delta_{\mathcal{R}}^2$. This can also be seen in Fig. 3. The dotted lines in Fig. 3 shows $-dP_{\kappa}^{ij}/d \ln \Delta_{\mathcal{R}}^2$, and this quantity exhibits a similar redshift and scale dependence as the derivatives of the spectra with respect to w_g . Though not shown, w_g is also strongly degenerate with ω_B . The net result of these degeneracies is that w_d will be significantly more strongly constrained by weak lensing power spectrum observations than w_g . This discussion is closely related to the eigenmode analysis of Ref. [16] and serves as a qualitative demonstration that both w_g and w_d can be constrained by cosmic shear measurements, but the relative constraints on each parameter are sensitive to choices for external priors in the available additional parameter space.

Having reviewed the influence of independent changes in the cosmological distance scale and the rate of density fluctuation growth on observable weak lensing power spectra, we now turn to projections for the utility of general relativity consistency checks. We utilized the split dark energy equation of state parameterization for the previous illustrations, but we present results for both the w_d - w_g parameterization as well as the growth index (γ) parameterization. Standard projections for the power of forthcoming consistency checks using weak lensing are summarized in Figure 4. Clearly such consistency checks can be quite powerful when definitive predictions can be made for the convergence power spectra. In the particular case of LSST, projected 1σ constraint on w_d is roughly $\sigma(w_d) \simeq 0.02$, while the projected constraint on the gravitational growth index is $\sigma(\gamma) \simeq 0.04$, meaning that the LSST weak lensing program alone could rule out DGP gravity at the $\sim 3.5\sigma$ level. In the case of the w_d - w_g parameterization, it is the equality of these two parameters that serves as a null hypothesis, so it is useful to look at the marginalized constraint on the combination $w_{\text{diff}} \equiv w_d - w_g$. Transforming to this variable, we find a 1σ constraint $\sigma(w_{\text{diff}}) = 0.04$ for LSST, $\sigma(w_{\text{diff}}) = 0.11$ for SNAP, and $\sigma(w_{\text{diff}}) = 0.14$ for DES.

Unfortunately, these standard projections assume perfect knowledge of nonlinear structure growth and ignore the influence of poorly-understood baryonic processes on the predictions of lensing spectra. Uncertainties due to baryonic processes and the

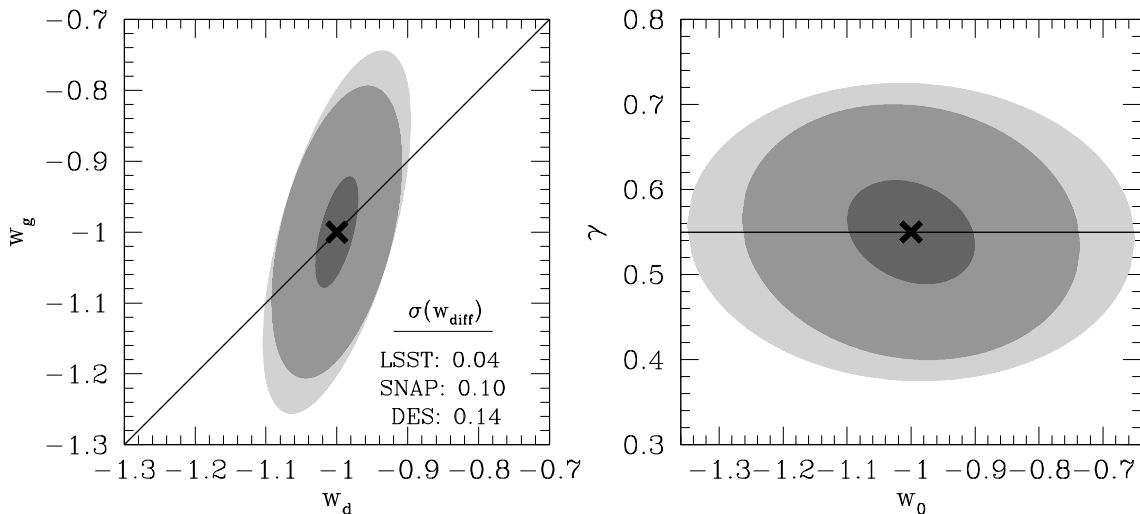


Figure 4: The capability of forthcoming surveys to perform consistency checks of general relativity. The *left* panel shows projected 1σ constraint contours in the w_d - w_g plane for the LSST (innermost contour), DES (outermost contour), and SNAP weak lensing (middle contour) experiments. The diagonal line in this panel delineates $w_g = w_d$. The constraints on the parameter $w_{\text{diff}} \equiv w_d - w_g$ from each experiment are given in the *lower, right* portion of the panel. The *right* panel shows constraints in the gravitational growth index parameterization in the w_0 - γ plane. The three contours represent the LSST, DES, and SNAP weak lensing experiments as in the *left* panel.

process of galaxy formation are significant and will be the subject of the remainder of this section, beginning with the following section where we demonstrate that such effects can significantly bias estimators of dark energy parameters and diminish the utility of consistency checks if not accounted for.

3.2 Biases

The poorly-constrained baryonic processes are detrimental to any consistency check of general relativity because, if unaccounted for, they may induce biases in inferred cosmological parameters. In particular, if the estimators of dark energy parameters that we have introduced are significantly biased, it would be possible to conclude erroneously that data are inconsistent with general relativity. The relevant quantities to examine in order to assess the importance of baryonic effects are the biases in units of the statistical uncertainties of those parameters. If the biases are small compared to the statistical uncertainties, it will be unlikely to rule out the true model based on these biases, but as biases become comparable to or larger than statistical uncertainties it becomes increasingly likely that the true model may be ruled out based on the data.

In practice it is difficult to estimate what biases may be realized, because the true

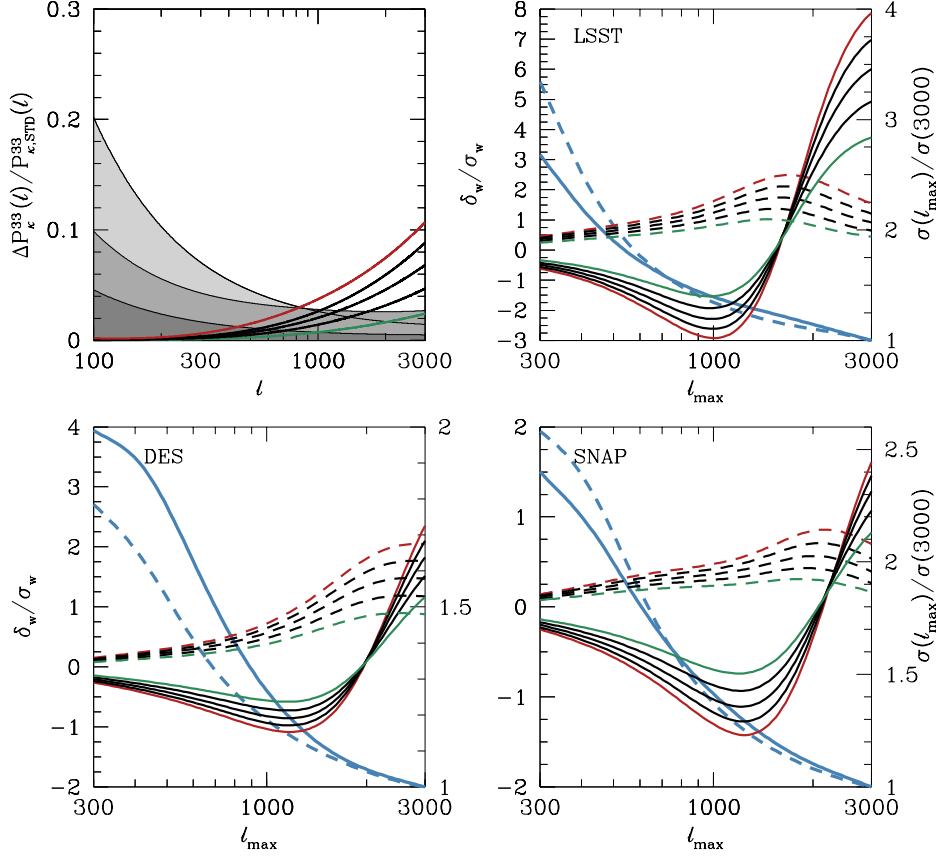


Figure 5: Biases in the estimators for the split dark energy parameters w_g and w_d that may be realized if baryonic processes are ignored. The *upper, left* panel shows the effect of modified halo structure on convergence power spectra. Each of the lines that increases with multipole represents the relative change in a convergence power spectrum of sources in our third tomographic bin ($1.2 \leq z_p < 1.8$) $P_\kappa^{33}(\ell)$, in models with modified halo structure relative to that of the standard case. We represent the standard case using a halo model where halo concentrations are given by Eq. (2.7) with $c_0 = 10$, $\alpha = 0.1$, and $\beta = 1.0$. We represent models with modified halo structure by taking $c_0 = 11, 12, 13, 14$, and, 15 from bottom to top. The shaded bands show the statistical errors on $P_\kappa^{33}(\ell)$ expected from forthcoming SNAP, DES, and LSST surveys from *top to bottom at left*. The other three panels show the biases in estimators w_d (*solid*) and w_g (*dashed*), in units of the statistical uncertainties in these parameters, as a function of the maximum multipole used in parameter estimation. These should be read against the *left* vertical axes. Each panel shows forecasts for a specific survey. The most biased cases correspond to $c_0 = 15$. The decreasing functions of ℓ_{\max} in each panel show the statistical uncertainty in w_d and w_g as a function of ℓ_{\max} relative to the error if all information to $\ell_{\max} = 3000$ were used. These lines should be read against the *right* vertical axes.

power spectra must be known in order to perform such a calculation (and, of course, if the true spectra were calculable there would be no bias). Fig. 5 gives an estimate of biases that may reasonably be realized for a variety of assumptions regarding the true convergence power spectra. We constructed these bias estimates as follows. Following the simulation analysis of Refs. [31], we assume that the primary influence of baryons can be accounted for in a halo model by adopting a non-standard halo concentration relation. It has been demonstrated that incorporating this additional freedom into the halo model enables accurate modeling of the results of non-radiative and dissipational hydrodynamic cosmological simulations and reduces expected biases in inferred dark energy parameters to acceptable levels [31]. The standard result for the concentration relation from gravity-only simulations is Eq. (2.7) with roughly $c_0 = 10$, $\alpha = 0.1$, and $\beta = 1.0$ [59]. We take this model to be our treatment of the results of N -body simulations. The halos in the simulations of Ref. [35] exhibit a $\sim 40\%$ enhancement in their concentrations in dissipational simulations relative to N -body simulations, so a choice of $c_0 \approx 14$ is an acceptable model for these simulation results. Unfortunately, our understanding of the evolution of baryons is poor and no simulation campaign can produce definitive results (it is this lack of definitiveness that is the primary problem). In particular, this boost is likely an over-estimate of any true shift due to galaxy formation because contemporary simulations exhibit baryonic cooling and star formation that is more efficient than allowed observationally [77, 78, 79, 80, 81]. As a consequence, baryonic processes must be treated in a way that accommodates a wide range of predictions. We illustrate reasonable levels of bias due to galaxy formation effects by computing the biases induced in dark energy parameter estimators when the convergence spectra are modeled with a fixed halo concentration-mass relation with $c_0 = 10$, but where the “true” value of this normalization ranges among $c_0 = 11, 12, 13, 14$, and, 15 . The lower end of this range is only a small shift relative to the standard concentration relation and is realized even in non-radiative hydrodynamic simulations where baryons cannot radiate their energy and form galaxies. The upper end of this range is slightly larger than the Ref. [35] simulation results and is near the maximum allowable by current lensing constraints at low redshift ($z \sim 0.2$) [82]. We note in passing that there are as yet weak observational indications of concentrations higher than those predicted by dissipationless simulations [83, 84].

Fig. 5 shows biases in the inferred w_g and w_d induced by treating convergence power spectra that would be well described by an enhanced concentration mass relation, where c_0 can be any of $c_0 = 11, 12, 13, 14$, or 15 , with a concentration-mass relation fixed to have $c_0 = 10$. The objective is to provide reasonable estimates for biases that may be realized by not treating baryonic processes appropriately. If the Ref. [35] simulation results were a good representation of the “true” convergence power spectra, the biases would be near the top of the range in Fig. 5, roughly corresponding to the fourth most strongly biased model in each panel.

To see why it is useful to consider biases in dark energy parameter estimators as a function of scale may require some elaboration. The influence of baryons is greater on smaller scales, so a simple way to eliminate the uncertainty caused by baryons is to excise small-scale information from parameter estimation. A simplistic way to do this is to choose a maximum multipole ℓ_{max} for the analysis and to disregard spectra beyond that maximum (Ref. [85] explores more sophisticated means to excise small-scale information, but they yield similar results in this context [31]). In Fig. 5, we show biases as a function of ℓ_{max} in order to illustrate the reduced biases realized as a function of minimum scale (maximum-multipole).

Fig. 5 illustrates several points of interest. Most previous lensing analysis have assumed that one could utilize information to at least $\ell_{\text{max}} \sim 10^3$ effectively. Fig. 5 shows that if one considers such small-scale information, estimators of dark energy equation of state parameters w_g and w_d will both be significantly biased relative to their true values. Notice also that they are generally biased in an *opposing* sense. This is of paramount importance for consistency checks where the goal is not necessarily to constrain either parameter individually, but to test the hypothesis that w_g and w_d are the same. For example, if w_g and w_d were always biased in the same way due to an unaccounted for systematic then it would not be possible to produce a reliable constraint on either parameter, but in this contrived example it would still be possible to test for their equality without accounting for the systematic. The biases in Fig. 5 are generally large compared to statistical uncertainties and suggest that consistency checks of general relativity can be compromised by uncertainty in galaxy formation physics and may lead to rejection of the hypothesis of general relativity even in models where this is the true theory of gravity. The point where biases become acceptable ($\delta_w \ll \sigma_w$) varies from one experiment to the next. One could argue that for the LSST survey these biases are not acceptable for any $\ell_{\text{max}} \gtrsim 300$.

As a rough criterion, Fig. 5 demonstrates that reducing the biases induced by the shifts in halo structure to acceptable levels requires taking a maximum multipole of no more than a few hundred. Of course, this reduction in information comes at a cost. The monotonically decreasing lines in Fig. 5 show the marginalized 1 σ statistical uncertainties in w_d and w_g as a function of the maximum multipole ℓ_{max} in units of the uncertainty when all information to an $\ell_{\text{max}} = 3000$ is used. Notice that these uncertainties should be read relative to the right vertical axes in each panel. Overlaying the dependence of parameter uncertainties on this plot serves to demonstrate the cost of excising small-scale information. For LSST, the cost is large, a factor of $\sim 3 - 4$ in the uncertainties of both w_d and w_g , because of the exquisite precision with which LSST could measure convergence spectra. This greatly reduces the effectiveness of an LSST-like data set to test the consistency of general relativity. DES is least affected by the uncertainty in galaxy formation because it surveys a comparably low number density of galaxies and makes the least use of small-scale information of any of the three experiments. SNAP is intermediate between the two

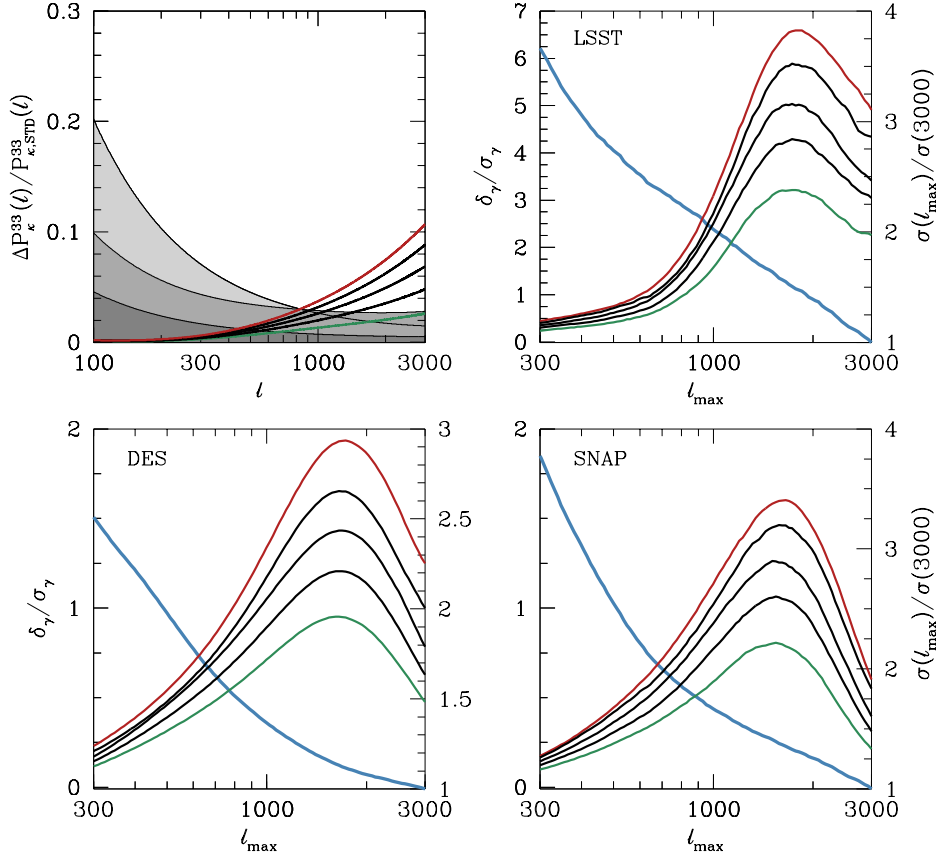


Figure 6: Estimates of biases in the estimator of the γ parameter of the gravitational growth index formalism proposed in Ref. [11]. The treatment of baryonic modifications to the convergence power spectrum is as in Fig. 5 and the *upper, left* panel is identical to the *upper, left* panel of Fig. 5. We repeat it here for convenience. The remaining panels show biases projected for the LSST, SNAP, and DES weak lensing surveys as indicated. Value of the biases should be read relative to the *left* vertical axes. The biases are given in units of the projected statistical uncertainty in γ and the most (least) biased case corresponds to a model with $c_0 = 15$ ($c_0 = 11$). The intermediate lines correspond to the intermediate values of c_0 with bias increasing with c_0 . The monotonically decreasing lines in each panel represent the 1σ statistical uncertainties in γ as a function of maximum multipole ℓ_{\max} . These are shown in units of the uncertainties in gamma achieved by considering all information to $\ell_{\max} = 3000$ in order to illustrate the relative degradation in constraints caused by excising small-scale information.

with constraints degraded by roughly a factor of ~ 2.5 .

Figure 6 shows the biased estimator for the gravitational growth index introduced in Ref. [11]. Our methods for computing biases and the presentation are analogous to that of Fig. 5. Of course, in this case the only parameter of importance is the

gravitational growth index γ . Qualitatively, Fig. 6 shows results that are similar to that of Fig. 5. In particular, biases can be considerable compared to statistical uncertainties. Moreover, excising small-scale information comes at great cost in the statistical uncertainties of the dark energy parameters, with relative degradation of $\sim 2 - 4$ depending upon the choice of ℓ_{max} and experimental parameters.

3.3 Calibration

In the previous section, we demonstrated the significance of the biases that would be induced in tests of general relativity if baryonic processes were to be ignored. We also showed the significant cost of excising information from the small scales where baryonic effects are most important in terms of degraded parameter uncertainties and thus degraded tests of the theory of gravity. What remains is to study whether such tests can still be performed utilizing high-multipole information if baryonic effects are treated in a parameterized way and calibrated simultaneously with the cosmological parameters. Though there is still significant work to be done, preliminary indications are that baryonic effects can indeed be treated by modifying the predictions of dissipationless N -body simulations [35, 35]. In fact, the necessary modification is to treat the relation between halo mass and halo concentration as free, and we have already utilized such modifications to estimate parameter biases in the previous section.

The next step is to determine the degree to which treating both halo structure and cosmology as uncertain, in order to eliminate the biases of the previous section, and fitting both to forthcoming data will degrade our ability to test general relativity. If the degradation is significantly less than that incurred by simply excising small-scale information, then an appropriate strategy to adopt in the run-up to the next generation of imaging surveys would be to spend significant effort understanding the phenomenology of structure growth in the nonlinear regime in a variety of different effective models for the evolution of the baryonic sector. It might then be possible to “self-calibrate” the influence of baryons, simultaneously yielding insight into the law of gravity on large scales and the small-scale physics of galaxy formation. Alternatively, if the degradation is comparable to the degradation incurred by excising small-scale information, such a program would likely be futile and it would be wiser to excise small-scale information until such time as definitive predictions for the influence of baryonic processes on lensing power spectra can be made.

There is already reason to be optimistic that some self-calibration can be achieved. Ref. [37] and Ref. [29] demonstrated the robustness of weak lensing to modest multiplicative and additive errors in shear measurements. In addition, Ref. [31] have already demonstrated robustness of weak lensing constraints on dark energy to some uncertainty in the power spectrum at high wavenumbers. A large part of potential to carry out self-calibration programs within weak lensing data can be gleaned from the eigenmode analysis of Ref. [16]. The robustness of weak lensing constraints on dark energy is due in part to the fact that weak lensing provides exquisite constraints on

distance measures that are relatively insensitive to dark energy and can be brought to bear on other systematics without degrading dark energy constraints.

In this section, we present the results of a self-calibration exercise where we treat cosmological parameters as before and introduce additional parameter freedom to describe the influence of baryons. To be specific, we treat the halo concentrations according to Eq. (2.7), but allow the parameters c_0 , α , and β to be free. It is already possible to offer a guess at the promise of such a self-calibration exercise. Fig. 3 shows the derivatives of three of our convergence power spectra P_κ^{22} , P_κ^{23} , and P_κ^{33} with respect to the parameters w_d , w_g , and $\ln \Delta_{\mathcal{R}}^2$. Compare this to the shifts in P_κ^{33} depicted in the upper, left panels of Fig. 5. Modifying the concentration relation causes significant increases in power at small scales (high multipoles). As a result, there is a stronger scale dependence associated with changes in concentration parameters than there is associated with changes to w_d , w_g , γ , or $\Delta_{\mathcal{R}}^2$. This is encouraging because it suggests that if the scale dependence can be adequately modeled, the parameters describing baryonic processes can be extracted independently without significantly degrading consistency checks of general relativity.

We show the results of the self-calibration exercise in Figure 7. In this panel we show constraints in the case of self calibration of halo structure $\sigma^{\text{self-cal}}(\ell_{\text{max}})$, in units of the parameter uncertainties that would be quoted in the standard case of perfect knowledge of halo structure, $\sigma^{\text{standard}}(\ell_{\text{max}})$ (shown in Fig. 4, Fig. 5, and Fig. 6). In particular, we show how the parameter degradation varies with ℓ_{max} because it is both instructive and it illustrates the balance between excising data and self-calibrating. Figure 7 shows results for both the w_d - w_g parameterization as well as the gravitational growth index (γ) parameterization.

It may seem odd that the functions in Fig. 7 do not decrease monotonically with increasing ℓ_{max} . These relations are not monotonic functions of ℓ_{max} because they represent the ratio of the error realized in the self-calibration calculation compared to the errors computed in the limit of perfect knowledge of the influence of baryons. From Fig. 5 and Fig. 6, the constraints on all parameters are rapidly decreasing functions of ℓ_{max} . This is sensible; as more information is added constraints should improve and not degrade. Likewise, in the case of self-calibration the absolute constraints on each parameter decrease rapidly with increasing ℓ_{max} . What is not monotonic is the relative degradation of these constraints as a function of ℓ_{max} .

The scale dependence of the parameter degradation is not surprising. From the power spectra in the upper, left panel of Fig. 5 and the derivatives in Fig. 3 it is evident that each of the parameters of interest induces a scale-dependence on the observed spectra, so some scales are more effective at constraining dark energy parameters and calibrating halo structure than others. Though the details depend upon the experiment, and in particular the statistical weight an experiment places on a particular multipole, there are sensible general trends depicted in Fig. 7. In the limit of low- ℓ , halo structure is unimportant and results in the self-calibration

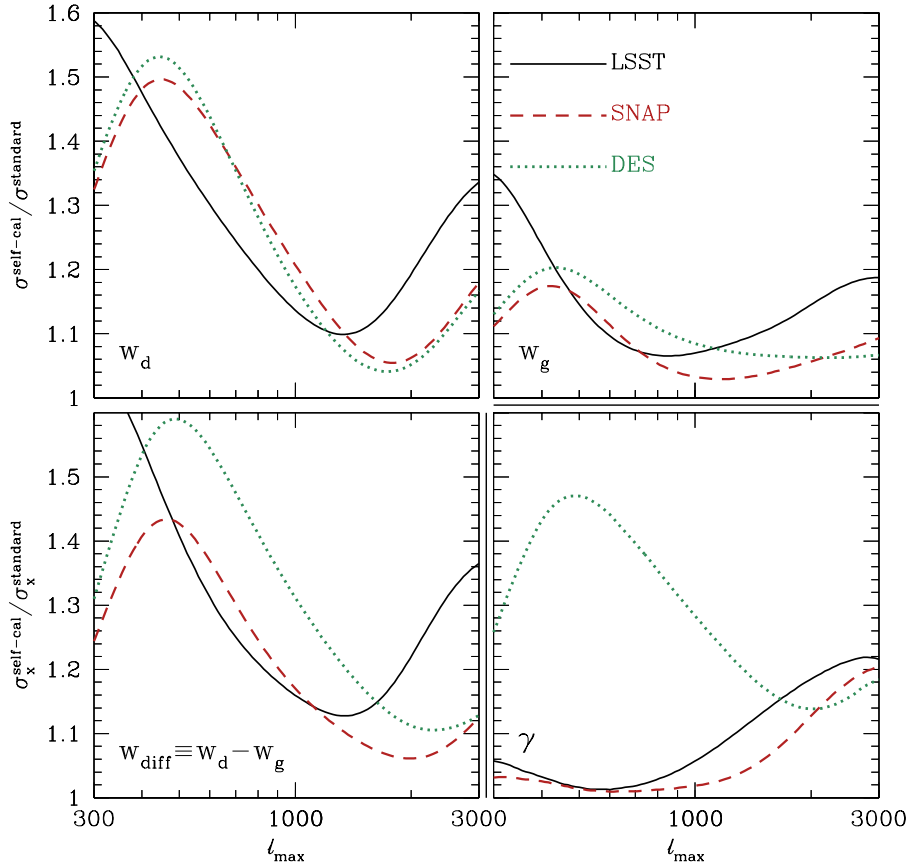


Figure 7: Results of self-calibrating halo structure simultaneously with tests for modified gravity on large scales. As with Fig. 5, we present results as a function of the maximum multipole considered in the parameter extraction analysis ℓ_{max} . The vertical axis is the error on the stated model parameter in the self-calibration case in units of $\sigma_X^{\text{standard}}$: the error on parameter X calculated by standard parameter forecasts that appear in the literature, where halo structure is assumed to be known perfectly. Each panel contains three lines for each set of experimental parameters we explore. The *solid* lines correspond to an LSST-like experiment, the *dashed* lines correspond to a SNAP-like experiment, and the *dotted* lines correspond to a DES-like experiment. Each panel focuses on a different parameter. The *upper, left* panel shows w_d , the *upper, right* panel shows w_g , the *bottom, left* panel shows the difference $w_{\text{diff}} = w_d - w_g$, and the *bottom, right* panel shows the gravitational growth index γ . Note that w_d and w_g are the parameters of our “dark energy split” model and are constrained simultaneously, and that the relevant constraint for tests of gravity is the constraint on w_{diff} . The γ parameter is from an entirely distinct parameterization in which dark energy is independently marginalized over. The additional lines that separate this panel from the others are intended to reinforce this distinction.

calculation approach the standard results. This is least evident for LSST because LSST has sufficient f_{sky} to make precise power spectrum measurements even for $\ell \sim 300$. We do not extend these plots to $\ell < 300$ because at this value of ℓ

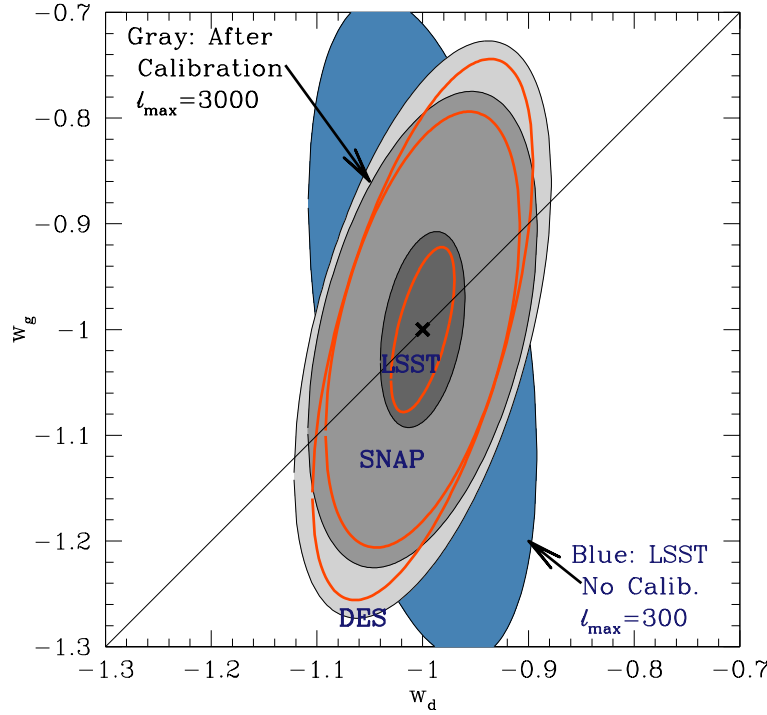


Figure 8: Constraint contours in the w_d - w_g plane after accounting for and marginalizing over the uncertainty in halo structure. The *filled, grey* contours correspond to the 1σ contours in this plane from the LSST-like (innermost contour), SNAP-like (middle contour), and DES-like (outermost blue contour) experiments we consider. The *thick, solid* lines overlaying the contours represent the confidence contours in the limit of perfect knowledge of nonlinear structure formation as shown in the left panel of Fig. 4. The cross shows the fiducial model and the diagonal line running from the lower left to the upper right delineates $w_d = w_g$. As an explicit demonstration of the effect of excising small-scale information to eliminate potential bias, the *outermost, blue* contour shows the 1σ marginalized constraint in the w_d - w_g plane from LSST if no information from multipoles greater than $\ell_{\max} = 300$ are utilized.

parameter biases are already at or near acceptable levels and so there is no need to relegate ourselves to such low multipoles in any data analysis. With increasing multipole, the halo structure becomes ever more important and is mildly degenerate with dark energy. Further increasing ℓ_{\max} beyond \sim several hundred introduces the strong scale dependence that halo structure imparts on the convergence spectra and this breaks a degeneracy between dark energy and halo structure. For this reason, the degradation decreases rapidly from $\ell_{\max} \sim 500$ to $\ell_{\max} \sim 2000$.

The most important aspect of Fig. 7 is that the degradations are relatively small if we utilize all of the information to $\ell_{\max} \gtrsim 10^3$. Degradations are scale dependent, but consider the level of degradation at $\ell_{\max} = 3000$ for definiteness. After calibrating halo structure, the w_d constraint is degraded by $\sim 34\%$ for LSST and roughly $\sim 18\%$ for DES and SNAP. The w_g constraint is degraded by $\sim 18\%$ for LSST and less than

10% for LSST and SNAP. The relevant combination $w_{\text{diff}} = w_{\text{d}} - w_{\text{g}}$ is degraded by a maximum of $\sim 36\%$ for LSST and only about $\sim 13\%$ for SNAP and DES. To appreciate the utility of self-calibration in this instance, we should compare these numbers to the information loss associated with excising small scale information in Fig. 5. For LSST, excising high- ℓ information to eliminate biases requires taking $\ell_{\text{max}} \sim 300$ with a corresponding $\sim 300\%$ increase in the constraints on w_{d} and w_{g} . So long as baryonic effects can be modeled in this way, the more sensible strategy is clearly to use all available information and calibrate the physics of galaxy formation as encoded in effective halo concentrations. The rightmost panel of Fig. 7 shows a similar result for the gravitational growth index γ . In particular, σ_{γ} is degraded by only $\sim 20\%$ after self calibration as compared to $\sim 200\%$ as would be required by the excision of small scales (see Fig. 6).

For completeness, we give a revised set of constraint contours in the $w_{\text{d}}-w_{\text{g}}$ plane in Fig. 8. After calibration, the contours are slightly expanded, but their orientation in this plane is only slightly changed. By comparison, eliminating small-scale information corresponds to a dramatic loss of constraining power both because the area of the constraint contour in the $w_{\text{d}}-w_{\text{g}}$ plane grows and because its orientation changes such that the most degenerate combination becomes more nearly perpendicular to the line $w_{\text{d}} = w_{\text{g}}$. The overall conclusion remains that self calibration is the appropriate strategy to adopt.

4. Discussion

We have extended recent studies of the influence of galaxy formation on weak lensing observables (in particular, Ref. [31]) to address cross-checks of the consistency of general relativity with weak lensing. Weak lensing is a key ingredient in such programs because weak lensing observables are sensitive to both the cosmological distance scale and the evolution of potential inhomogeneities, whereas the Type Ia supernovae distance-redshift relation and baryonic acoustic oscillation measurements are sensitive only to geometry (though it may be possible to exploit the lensing of supernovae while performing the distance-redshift test, see Refs. [86, 87, 88] or to combine distance measures with cluster counts). Proposed methods to utilize weak lensing to constrain dark energy and to place limits on deviations from general relativity on cosmological scales assume that correlations on scales as small as a few arcminutes ($\ell \sim 10^3$) can be brought to bear on the cause of cosmic acceleration. Such small-scale information is important to these programs. Relegating consideration to larger scales can significantly degrade the constraining power of forthcoming experiments (see Fig. 5 and Fig. 6) by nearly a factor of ~ 3 decrease in the effectiveness of tests for deviations from general relativity.

One of the anticipated challenges of using this small-scale information is that it is difficult to predict observables on these scales because the physics that governs

the evolution of the baryonic component of the Universe is poorly understood and affects these observables in important ways [32, 33, 34, 35]. In Fig. 5 and Fig. 6, we show that using such data to test general relativity may introduce potentially large biases in the inferred values of cosmological parameters that can lead to ruling out general relativity when it is in fact the true theory of gravitation. In these figures, we give a range of estimates of potential biases that may be realized. These results are motivated by the specific results of the simulations of [35]. The biases can be many times the statistical uncertainties in these parameters, which is clearly a serious problem. We reiterate here that we give a range of biases that may be realized precisely because it is difficult to predict the precise influences of baryons. We have used simulation results as guidance and explored a range of concentration relations that are consistent with current observations (e.g., Ref. [82]). We have not included information from additional observables that can be brought to bear on this problem. For example, supernova Ia and baryon acoustic oscillation data can constrain the cosmic distance-redshift relation and be combined with lensing to produce stronger consistency checks. However, these additional constraints on cosmological distances would only make the discord between structure growth and distance measures more egregious and drive larger biases, making the problem more severe.

Faced with a large systematic error, a common practice is to degrade the experiment in some way so as to derive robust results from the data and reduce sensitivity to the systematic error. Baryonic influences are scale dependent, so one way to degrade the experiment and eliminate these biases is to disregard small-scale information by restricting the analysis to $\ell_{\text{max}} \sim \text{a few} \times 10^2$. However, in Fig. 5 we have shown that this comes at the cost of nearly a factor of ~ 3 decrease in the effectiveness of tests for deviations from general relativity (more sophisticated analyses, such as those in Ref. [85], yield similar results).

As an alternative to excising small scale information, simulations suggest that we can understand the form of the baryonic influence and correct for it using a parameterized model. To the degree that this form is not exactly degenerate with parameterizations of dark energy or deviations from general relativity, this enables the utilization of some of the information on small scales. We addressed these biases by including 3 baryonic parameters, α, β , and c_0 , that model the effective concentration of dark matter halos as specified in Eq. 2.7. This choice of parametrization is motivated by Refs. [35, 31], wherein the authors demonstrated that modifying halo concentrations allows one to model account for the net influences of baryonic processes on scales relevant to weak lensing parameter estimation. In particular, models in which the N -body results are corrected by a modified halo concentration relation track the convergence spectra from galaxy formation simulations out to $\ell \sim 5000$ accurately enough to reduce the biases in inferred dark energy parameters to levels below the statistical uncertainty of forthcoming experiments. Within this

framework, we studied the ability of forthcoming imaging surveys to self-calibrate the values of the baryonic parameters and simultaneously use this information to check the consistency of general relativity.

In Fig. 7 we have illustrated the effectiveness of our method by using the Fisher Matrix formalism to estimate the constraints on γ and $w_g - w_d$ that will be obtained from future photometric surveys. From this figure, it is evident that the constraints on the consistency of general relativity degrade by just $\sim 30\%$ relative to the limit of perfect knowledge of nonlinear evolution of the gravitational potential. In Fig. 8 the constraints on the consistency of general relativity obtained through our methods are much tighter than those from analyses excising small scale information. In light of our findings, we conclude that self-calibration of some of the specific influences of baryonic physics may be an appealing alternative to disregarding the information contained on scales smaller than $\ell \sim 300$.

Our outlook for self-calibration of uncertain baryonic physics is quite positive; however, there are several important caveats to our study and a number of additional studies that must be undertaken in order to bring such a program to fruition. First, this correction for the physics of galaxy formation has only been applied to the simulations of Ref. [35]. As the physics of baryons is highly uncertain, a more comprehensive exploration of viable alternative models is needed in order to validate such a correction term. In fact, it is not reasonable to suppose that the influences of baryons should be strictly confined to the internal structures of halos (see Ref. [89] for changes in the halo mass function) and other effects may prove important. Nevertheless, our study indicates that such an exploration is a fruitful pursuit.

Second, any such tests have important limitations. The self-calibration program that we have explored should guard against the possibility of ruling out general relativity when it is the correct theory of gravity. In our particular study, we have not explored complete, self-consistent phenomenologies for modified gravity. Rather, we have only explored proposals that are already in the literature in which additional parameters are introduced which have known, fixed values in general relativity and explored the ability of forthcoming surveys to constrain these parameters. In the event of a detection of a deviation from general relativity such tests provide limited information about the character of the correct, alternative theory. In large part, this is due to the fact that modified gravity models must have some scale dependence so that they can simultaneously drive accelerated cosmic expansion yet satisfy small-scale bounds on the theory of gravity [61, 62, 63, 64, 65, 66, 67]. If a modified gravity theory, including nonlinear evolution, were fully specified and explored and if galaxy formation processes were more completely understood, it would be possible to draw more specific conclusions from forthcoming imaging survey data.

Lastly, we note that we operate under the assumption that dissipationless N -body simulations will effectively calibrate the properties of the lensing field absent baryonic effects. In our halo model approach, this is tantamount to a calibration of

dark matter halo abundance and halo clustering that is so accurate as to introduce negligible uncertainties. This is a common premise to all such studies of dark energy constraints as it is known that the density field is not yet calibrated with sufficient accuracy to analyze forthcoming data [36, 43, 44]. Our outlook is that it is plausible that a brute force simulation campaign can achieve sufficient accuracy in this regard, though it is certainly possible that reaching this goal may be complicated by several factors that have not yet been thoroughly studied. For example, the phenomenologies we explore here are relatively simple, as they treat modified gravity only as a modification to the growth function. Ultimately, it will be of interest to study more specific and more complete phenomenological models of modified gravity that may lead to large corrections to the density field on scales of several Mpc. Additionally, even in the absence of corrections necessitated by modified gravity it is possible that a program of N -body simulations coupled with a calibration of baryonic effects may encounter unforeseen obstacles. In either case, the assumption that an adequate suite of N -body simulations will address the density field (in our parameterization halo bias and halo abundance) with sufficient precision so as to render errors in the predicted density field negligible in the dissipationless case may not be valid. In such cases, it would be necessary to allow for adequate model freedom to account for this uncertainty. In the language of our paper, this might amount to internal calibration of halo abundance and halo bias (presumably with significant prior information) as well. Such additional freedom would lead to further degradation in dark energy and/or modified gravity parameters. We have chosen to limit the scope of our work along these lines and not studied this more complicated case.

5. Summary

We have explored the ability of forthcoming weak lensing surveys to perform a consistency check on general relativity as the correct theory of gravity in light of recent uncertainties in predicting lensing observables on scales smaller than ~ 10 arcmin due to the poorly-understood evolution of the baryonic component of the Universe. After a pedagogical demonstration of the utility of such consistency checks in § 3.1, we present the following results.

1. Conducting a study of the consistency of general relativity by analyzing weak lensing observables from a forthcoming imaging survey (such as DES, JDEM/SNAP, or LSST) out to scales as small as $\ell \sim 10^3$ could potentially lead to inferred cosmological parameters that are biased by many times the statistical uncertainty of such surveys if baryonic effects on the nonlinear evolution of the gravitational potential are ignored. The problem is severe in that *they could lead to rejection of the null hypothesis of general relativistic gravity, even when it is*

the true theory. Specific results depend upon the assumed survey properties and the importance of baryonic processes.

2. Disregarding small-scale information beyond $\ell \sim \text{a few} \times 10^2$ significantly reduces these biases because of the strong scale-dependence of the influence of baryonic physics on weak lensing observables. However, excising this information degrades the constraining power of forthcoming imaging surveys by a factor of ~ 3 .
3. As an alternative to excising small-scale information, we explore a program of self-calibrating a phenomenological model of baryonic processes that is motivated by recent numerical simulations. With such a model small-scale information out to $\ell \sim 10^3$ can be exploited, and biases can be reduced to levels below those of the statistical uncertainty of forthcoming experiments. As shown in Fig. 7 and Fig. 8, this method provides substantially tighter constraints on the consistency of general relativity than analyses that disregard small-scale information.
4. The program to calibrate the baryonic correction internally allows small-scale information to be used to constrain gravity and guards against ruling out general relativity when it is the true theory. In the case of internal calibration, the limits provided by general relativity consistency checks are degraded by only $\sim 30\%$ relative to the limits that would be achieved if nonlinear structure formation were perfectly understood. Moreover, interesting limits on galaxy formation models are produced as a “byproduct.”

These results should be carefully considered in preparation for the weak lensing surveys that will be conducted in the next decade. At the very least, it should be clear that issues regarding the baryonic influences on lensing observables will need to be dealt with, but that uncertainty in this regime may not necessarily have dramatic consequences on the ability of imaging surveys to illuminate the cause of cosmic acceleration. It seems likely that a program of internal calibration of baryonic physics will allow lensing surveys to achieve stringent limits on gravity and dark energy. In order to ensure that this is the case, a comprehensive theoretical program will need to be undertaken to better understand viable alternatives for the net influences of baryons on observable power spectra.

Acknowledgments

We thank Wayne Hu, Dragan Huterer, Manoj Kaplinghat, Arthur Kosowsky, Andrey Kravtsov, Jeff Newman, Douglas Rudd, and Mel Sanger for useful discussions. ARZ and APH are supported by the University of Pittsburgh, by the US National Science Foundation through grant AST 0806367, and by the US Department of Energy.

References

- [1] A. G. Riess, A. V. Filippenko, P. Challis, and et al., *Observational Evidence from Supernovae for an Accelerating Universe and a Cosmological Constant*, *Astron. J.* **116** (Sept., 1998) 1009–1038, [astro-ph/9805201].
- [2] S. Perlmutter, G. Aldering, G. Goldhaber, and et al., *Measurements of Omega and Lambda from 42 High-Redshift Supernovae*, *Astrophys. J.* **517** (June, 1999) 565–586, [astro-ph/9812133].
- [3] M. Tegmark, M. A. Strauss, M. R. Blanton, and et al., *Cosmological parameters from SDSS and WMAP*, *Phys. Rev. D* **69** (May, 2004) 103501, [astro-ph/0310723].
- [4] A. G. Riess, L.-G. Strolger, J. Tonry, S. Casertano, H. C. Ferguson, B. Mobasher, P. Challis, A. V. Filippenko, S. Jha, W. Li, R. Chornock, R. P. Kirshner, B. Leibundgut, M. Dickinson, M. Livio, M. Giavalisco, C. C. Steidel, T. Benítez, and Z. Tsvetanov, *Type Ia Supernova Discoveries at $z \lesssim 1$ from the Hubble Space Telescope: Evidence for Past Deceleration and Constraints on Dark Energy Evolution*, *Astrophys. J.* **607** (June, 2004) 665–687, [astro-ph/0402512].
- [5] D. J. Eisenstein, I. Zehavi, D. W. Hogg, and et al., *Detection of the Baryon Acoustic Peak in the Large-Scale Correlation Function of SDSS Luminous Red Galaxies*, *Astrophys. J.* **633** (Nov., 2005) 560–574, [astro-ph/0501171].
- [6] D. N. Spergel, R. Bean, O. Doré, M. R. Nolta, C. L. Bennett, J. Dunkley, G. Hinshaw, N. Jarosik, E. Komatsu, L. Page, H. V. Peiris, L. Verde, M. Halpern, R. S. Hill, A. Kogut, M. Limon, S. S. Meyer, N. Odegard, G. S. Tucker, J. L. Weiland, E. Wollack, and E. L. Wright, *Three-Year Wilkinson Microwave Anisotropy Probe (WMAP) Observations: Implications for Cosmology*, *Astrophys. J. Supp. Ser.* **170** (June, 2007) 377–408, [astro-ph/].
- [7] M. Tegmark, D. J. Eisenstein, M. A. Strauss, and et al., *Cosmological constraints from the SDSS luminous red galaxies*, *Phys. Rev. D* **74** (Dec., 2006) 123507, [astro-ph/0608632].
- [8] P. Astier, J. Guy, N. Regnault, and et al., *The Supernova Legacy Survey: measurement of Ω_M , Ω_Λ and w from the first year data set*, *Astron. Astrophys.* **447** (Feb., 2006) 31–48, [astro-ph/0510447].
- [9] W. M. Wood-Vasey, G. Miknaitis, C. W. Stubbs, and et al., *Observational Constraints on the Nature of the Dark Energy: First Cosmological Results from the ESSENCE Supernova Survey*, *Astrophys. J. submitted (astro-ph/0701041)* (Jan., 2007) [astro-ph/0701041].
- [10] J. Zhang, L. Hui, and A. Stebbins, *Isolating geometry in weak lensing measurements*, *Astrophys. J.* **635** (2005) 806–820, [astro-ph/0312348].

- [11] E. V. Linder, *Cosmic growth history and expansion history*, *Phys. Rev. D* **72** (Aug., 2005) 043529–+, [[astro-ph/](#)].
- [12] H. Zhan and L. Knox, *How Tomographic Cosmic Shear Maps Lead to Constraints on Dark Energy Properties*, *ArXiv Astrophysics e-prints* (Nov., 2006) [[astro-ph/](#)].
- [13] S. Wang, L. Hui, M. May, and Z. Haiman, *Is modified gravity required by observations? An empirical consistency test of dark energy models*, *Phys. Rev. D* **76** (Sept., 2007) 063503–+, [[arXiv:0705.0165](#)].
- [14] D. Huterer and E. V. Linder, *Separating dark physics from physical darkness: Minimalist modified gravity versus dark energy*, *Phys. Rev. D* **75** (Jan., 2007) 023519–+, [[astro-ph/](#)].
- [15] E. V. Linder and R. N. Cahn, *Parameterized beyond-Einstein growth*, *Astroparticle Physics* **28** (Dec., 2007) 481–488, [[astro-ph/](#)].
- [16] H. Zhan, L. Knox, and J. A. Tyson, *Distance, Growth Factor, and Dark Energy Constraints from Photometric Baryon Acoustic Oscillation and Weak Lensing Measurements*, *ArXiv e-prints* (June, 2008) [[arXiv:0806.0937](#)].
- [17] M. J. Mortonson, W. Hu, and D. Huterer, *Falsifying Paradigms for Cosmic Acceleration*, *ArXiv e-prints* (Oct., 2008) [[arXiv:0810.1744](#)].
- [18] W. Hu and M. Tegmark, *Weak Lensing: Prospects for Measuring Cosmological Parameters*, *Astrophys. J. Lett.* **514** (Apr., 1999) L65–L68, [[astro-ph/9811168](#)].
- [19] W. Hu, *Power Spectrum Tomography with Weak Lensing*, *Astrophys. J. Lett.* **522** (Sept., 1999) L21–L24, [[astro-ph/9904153](#)].
- [20] D. Huterer, *Weak lensing and dark energy*, *Phys. Rev. D* **65** (Mar., 2002) 063001, [[astro-ph/0106399](#)].
- [21] A. Heavens, *3D weak lensing*, *Mon. Not. R. Astron. Soc.* **343** (Aug., 2003) 1327–1334, [[astro-ph/0304151](#)].
- [22] A. Refregier, *Weak Gravitational Lensing by Large-Scale Structure*, *Ann. Rev. Astron. Astrophys.* **41** (2003) 645–668, [[astro-ph/0307212](#)].
- [23] A. Refregier, R. Massey, J. Rhodes, R. Ellis, J. Albert, D. Bacon, G. Bernstein, T. McKay, and S. Perlmutter, *Weak Lensing from Space. III. Cosmological Parameters*, *Astron. J.* **127** (June, 2004) 3102–3114, [[astro-ph/0304419](#)].
- [24] Y.-S. Song and L. Knox, *Determination of cosmological parameters from cosmic shear data*, *Phys. Rev. D* **70** (Sept., 2004) 063510, [[astro-ph/0312175](#)].
- [25] M. Takada and B. Jain, *Cosmological parameters from lensing power spectrum and bispectrum tomography*, *Mon. Not. R. Astron. Soc.* **348** (Mar., 2004) 897–915, [[astro-ph/0310125](#)].

- [26] M. Takada and M. White, *Tomography of Lensing Cross-Power Spectra*, *Astrophys. J. Lett.* **601** (Jan., 2004) L1–L4, [astro-ph/0311104].
- [27] G. M. Bernstein and B. Jain, *Dark energy constraints from weak lensing cross-correlation cosmography*, *Astrophys. J.* **600** (2004) 17–25, [astro-ph/0309332].
- [28] S. Dodelson and P. Zhang, *Weak lensing bispectrum*, *Phys. Rev. D* **72** (Oct., 2005) 083001, [astro-ph/0501063].
- [29] A. Albrecht, G. Bernstein, R. Cahn, W. L. Freedman, J. Hewitt, W. Hu, J. Huth, M. Kamionkowski, E. W. Kolb, L. Knox, J. C. Mather, S. Staggs, and N. B. Suntzeff, *Report of the Dark Energy Task Force*, (astro-ph/0609591) (Sept., 2006) [astro-ph/0609591].
- [30] H. Zhan, *Cosmic tomographies: baryon acoustic oscillations and weak lensing*, *Journal of Cosmology and Astro-Particle Physics* **8** (Aug., 2006) 8, [astro-ph/0605696].
- [31] A. R. Zentner, D. H. Rudd, and W. Hu, *Self-calibration of tomographic weak lensing for the physics of baryons to constrain dark energy*, *Phys. Rev. D* **77** (Feb., 2008) 043507–+, [0709.4029].
- [32] M. White, *Baryons and weak lensing power spectra*, *Astroparticle Physics* **22** (Nov., 2004) 211–217, [astro-ph/0405593].
- [33] H. Zhan and L. Knox, *Effect of Hot Baryons on the Weak-Lensing Shear Power Spectrum*, *Astrophys. J. Lett.* **616** (Dec., 2004) L75–L78, [astro-ph/0409198].
- [34] Y. P. Jing, P. Zhang, W. P. Lin, L. Gao, and V. Springel, *The Influence of Baryons on the Clustering of Matter and Weak-Lensing Surveys*, *Astrophys. J. Lett.* **640** (Apr., 2006) L119–L122, [astro-ph/0512426].
- [35] D. H. Rudd, A. R. Zentner, and A. V. Kravtsov, *Effects of Baryons and Dissipation on the Matter Power Spectrum*, *Astrophys. J.* **672** (Mar., 2007) 19, [astro-ph/0703741].
- [36] D. Huterer and M. Takada, *Calibrating the nonlinear matter power spectrum: Requirements for future weak lensing surveys*, *Astroparticle Physics* **23** (May, 2005) 369–376, [astro-ph/0412142].
- [37] D. Huterer, M. Takada, G. Bernstein, and B. Jain, *Systematic errors in future weak-lensing surveys: requirements and prospects for self-calibration*, *Mon. Not. R. Astron. Soc.* **366** (Feb., 2006) 101–114, [astro-ph/0506030].
- [38] K. Heitmann, P. M. Ricker, M. S. Warren, and S. Habib, *Robustness of Cosmological Simulations. I. Large-Scale Structure*, *Astrophys. J. Supp. Ser.* **160** (Sept., 2005) 28–58, [astro-ph/0411795].

- [39] K. Heitmann, Z. Lukić, P. Fasel, S. Habib, M. S. Warren, M. White, J. Ahrens, L. Ankeny, R. Armstrong, B. O’Shea, P. M. Ricker, V. Springel, J. Stadel, and H. Trac, *The cosmic code comparison project, Computational Science and Discovery* **1** (Oct., 2008) 015003–+, [[arXiv:0706.1270](#)].
- [40] K. Heitmann, M. White, C. Wagner, S. Habib, and D. Higdon, *The Coyote Universe I: Precision Determination of the Nonlinear Matter Power Spectrum, ArXiv e-prints* (Dec., 2008) [[arXiv:0812.1052](#)].
- [41] K. Heitmann, D. Higdon, M. White, S. Habib, B. J. Williams, and C. Wagner, *The Coyote Universe II: Cosmological Models and Precision Emulation of the Nonlinear Matter Power Spectrum, ArXiv e-prints* (Feb., 2009) [[arXiv:0902.0429](#)].
- [42] Z. Lukić, K. Heitmann, S. Habib, S. Bashinsky, and P. M. Ricker, *The Halo Mass Function: High-Redshift Evolution and Universality, Astrophys. J.* **671** (Dec., 2007) 1160–1181, [[astro-ph/](#)].
- [43] J. Tinker, A. V. Kravtsov, A. Klypin, K. Abazajian, M. Warren, G. Yepes, S. Gottlöber, and D. E. Holz, *Toward a Halo Mass Function for Precision Cosmology: The Limits of Universality, Astrophys. J.* **688** (Dec., 2008) 709–728, [[arXiv:0803.2706](#)].
- [44] B. Robertson, A. Kravtsov, J. Tinker, and A. Zentner, *Collapse Barriers and Halo Abundance: Testing the Excursion Set Ansatz, ArXiv e-prints* (Dec., 2008) [[arXiv:0812.3148](#)].
- [45] Z. Ma, W. Hu, and D. Huterer, *Effects of Photometric Redshift Uncertainties on Weak-Lensing Tomography, Astrophys. J.* **636** (Jan., 2006) 21–29, [[astro-ph/0506614](#)].
- [46] M. White and W. Hu *Astrophys. J.* **537** (2000) 1.
- [47] A. Cooray and W. Hu, *Power Spectrum Covariance of Weak Gravitational Lensing, Astrophys. J.* **554** (June, 2001) 56–66, [[astro-ph/0012087](#)].
- [48] C. Vale and M. White *Astrophys. J.* **592** (2003) 699.
- [49] S. Dodelson, C. Shapiro, and M. White, *Reduced shear power spectrum, Phys. Rev. D* **73** (Jan., 2006) 023009–+, [[astro-ph/](#)].
- [50] E. Semboloni, L. van Waerbeke, C. Heymans, T. Hamana, S. Colombi, M. White, and Y. Mellier, *Cosmic variance of weak lensing surveys in the non-Gaussian regime, Mon. Not. R. Astron. Soc.* **375** (Feb., 2007) L6–L10, [[astro-ph/](#)].
- [51] R. J. Scherrer and E. Bertschinger, *Statistics of primordial density perturbations from discrete seed masses, Astrophys. J.* **381** (Nov., 1991) 349–360.
- [52] C.-P. Ma and J. N. Fry, *Deriving the Nonlinear Cosmological Power Spectrum and Bispectrum from Analytic Dark Matter Halo Profiles and Mass Functions, Astrophys. J.* **543** (Nov., 2000) 503–513, [[astro-ph/0003343](#)].

- [53] U. Seljak, *Analytic model for galaxy and dark matter clustering*, *Mon. Not. R. Astron. Soc.* **318** (Oct., 2000) 203–213.
- [54] A. Cooray and R. Sheth, *Halo models of large scale structure*, *Phys. Rep.* **372** (Dec., 2002) 1–129.
- [55] R. K. Sheth and G. Tormen, *Large-scale bias and the peak background split*, *Mon. Not. R. Astron. Soc.* **308** (Sept., 1999) 119–126, [astro-ph/9901122].
- [56] J. F. Navarro, C. S. Frenk, and S. D. M. White, *A Universal Density Profile from Hierarchical Clustering*, *Astrophys. J.* **490** (Dec., 1997) 493, [astro-ph/9611107].
- [57] J. S. Bullock, T. S. Kolatt, Y. Sigad, R. S. Somerville, A. V. Kravtsov, A. A. Klypin, J. R. Primack, and A. Dekel, *Profiles of dark haloes: evolution, scatter and environment*, *Mon. Not. R. Astron. Soc.* **321** (Mar., 2001) 559–575, [astro-ph/9908159].
- [58] A. V. Macciò, A. A. Dutton, F. C. van den Bosch, B. Moore, D. Potter, and J. Stadel, *Concentration, spin and shape of dark matter haloes: scatter and the dependence on mass and environment*, *Mon. Not. R. Astron. Soc.* **378** (June, 2007) 55–71, [astro-ph/].
- [59] A. F. Neto, L. Gao, P. Bett, S. Cole, J. F. Navarro, C. S. Frenk, S. D. M. White, V. Springel, and A. Jenkins, *The statistics of LCDM Halo Concentrations*, *ArXiv e-prints* **706** (June, 2007) [arXiv:0706.2919].
- [60] D. Dolney, B. Jain, and M. Takada, *Effects of halo substructure on the power spectrum and bispectrum*, *Mon. Not. R. Astron. Soc.* **352** (Aug., 2004) 1019–1027, [astro-ph/].
- [61] J. Khoury and A. Weltman, *Chameleon Fields: Awaiting Surprises for Tests of Gravity in Space*, *Physical Review Letters* **93** (Oct., 2004) 171104–+, [astro-ph/].
- [62] J. Khoury and A. Weltman, *Chameleon cosmology*, *Phys. Rev. D* **69** (Feb., 2004) 044026–+, [astro-ph/].
- [63] I. Navarro and K. Van Acoleyen, *Modified gravity, dark energy and modified Newtonian dynamics*, *Journal of Cosmology and Astro-Particle Physics* **9** (Sept., 2006) 6–+, [gr-qc/051].
- [64] I. Navarro and K. Van Acoleyen, *$f(R)$ actions, cosmic acceleration and local tests of gravity*, *Journal of Cosmology and Astro-Particle Physics* **2** (Feb., 2007) 22–+, [gr-qc/061].
- [65] T. Faulkner, M. Tegmark, E. F. Bunn, and Y. Mao, *Constraining $f(R)$ gravity as a scalar-tensor theory*, *Phys. Rev. D* **76** (Sept., 2007) 063505–+, [astro-ph/].
- [66] W. Hu and I. Sawicki, *Models of $f(R)$ cosmic acceleration that evade solar system tests*, *Phys. Rev. D* **76** (Sept., 2007) 064004–+, [arXiv:0705.1158].

- [67] H. Oyaizu, M. Lima, and W. Hu, *Non-linear evolution of $f(R)$ cosmologies II: power spectrum*, *ArXiv e-prints* (July, 2008) [[arXiv:0807.2462](#)].
- [68] J. M. Bardeen, P. J. Steinhardt, and M. S. Turner, *Spontaneous creation of almost scale-free density perturbations in an inflationary universe*, *Phys. Rev. D* **28** (Aug., 1983) 679–693.
- [69] D. H. Lyth, *Large-scale energy-density perturbations and inflation*, *Phys. Rev. D* **31** (Apr., 1985) 1792–1798.
- [70] V. F. Mukhanov, H. A. Feldman, and R. H. Brandenberger, *Theory of cosmological perturbations*, *Phys. Rep.* **215** (June, 1992) 203–333.
- [71] C.-P. Ma and E. Bertschinger, *Cosmological Perturbation Theory in the Synchronous and Conformal Newtonian Gauges*, *Astrophys. J.* **455** (Dec., 1995) 7–+, [[astro-ph/](#)].
- [72] W. Hu and I. Sawicki, *Parametrized post-Friedmann framework for modified gravity*, *Phys. Rev. D* **76** (Nov., 2007) 104043–+, [[arXiv:0708.1190](#)].
- [73] G. Dvali, G. Gabadadze, and M. Porrati, *4D gravity on a brane in 5D Minkowski space*, *Physics Letters B* **485** (July, 2000) 208–214, [[hep-th/00](#)].
- [74] W. Fang, S. Wang, W. Hu, Z. Haiman, L. Hui, and M. May, *Challenges to the DGP Model from Horizon-Scale Growth and Geometry*, *ArXiv e-prints* (Aug., 2008) [[arXiv:0808.2208](#)].
- [75] M. Chevallier and D. Polarski, *Accelerating Universes with Scaling Dark Matter*, *International Journal of Modern Physics D* **10** (2001) 213–223, [[gr-qc/000](#)].
- [76] E. Komatsu, J. Dunkley, M. R. Nolte, C. L. Bennett, B. Gold, G. Hinshaw, N. Jarosik, D. Larson, M. Limon, L. Page, D. N. Spergel, M. Halpern, R. S. Hill, A. Kogut, S. S. Meyer, G. S. Tucker, J. L. Weiland, E. Wollack, and E. L. Wright, *Five-Year Wilkinson Microwave Anisotropy Probe (WMAP) Observations: Cosmological Interpretation*, *ArXiv e-prints* (Mar., 2008) [[arXiv:0803.0547](#)].
- [77] N. Katz and S. D. M. White, *Hierarchical galaxy formation - Overmerging and the formation of an X-ray cluster*, *Astrophys. J.* **412** (Aug., 1993) 455–478.
- [78] G. F. Lewis, A. Babul, N. Katz, T. Quinn, L. Hernquist, and D. H. Weinberg, *The Effects of Gasdynamics, Cooling, Star Formation, and Numerical Resolution in Simulations of Cluster Formation*, *Astrophys. J.* **536** (June, 2000) 623–644, [[astro-ph/9907097](#)].
- [79] F. R. Pearce, P. A. Thomas, H. M. P. Couchman, and A. C. Edge, *The effect of radiative cooling on the X-ray properties of galaxy clusters*, *Mon. Not. R. Astron. Soc.* **317** (Oct., 2000) 1029–1040, [[astro-ph/9908062](#)].
- [80] M. L. Balogh, F. R. Pearce, R. G. Bower, and S. T. Kay, *Revisiting the cosmic cooling crisis*, *Mon. Not. R. Astron. Soc.* **326** (Oct., 2001) 1228–1234, [[astro-ph/0104041](#)].

- [81] T. Suginohara and J. P. Ostriker, *The Effect of Cooling on the Density Profile of Hot Gas in Clusters of Galaxies: Is Additional Physics Needed?*, *Astrophys. J.* **507** (Nov., 1998) 16–23, [[astro-ph/9803318](#)].
- [82] R. Mandelbaum, U. Seljak, and C. M. Hirata, *A halo mass–concentration relation from weak lensing*, *Journal of Cosmology and Astro-Particle Physics* **8** (Aug., 2008) 6–+, [[arXiv:0805.2552](#)].
- [83] D. A. Buote, F. Gastaldello, P. J. Humphrey, L. Zappacosta, J. S. Bullock, F. Brighenti, and W. G. Mathews, *The X-Ray Concentration-Virial Mass Relation*, (*astro-ph/0610135*) (Oct., 2006) [[astro-ph/0610135](#)].
- [84] A. Vikhlinin, A. Kravtsov, W. Forman, C. Jones, M. Markevitch, S. S. Murray, and L. Van Speybroeck, *Chandra Sample of Nearby Relaxed Galaxy Clusters: Mass, Gas Fraction, and Mass-Temperature Relation*, *Astrophys. J.* **640** (Apr., 2006) 691–709, [[astro-ph/0507092](#)].
- [85] D. Huterer and M. White, *Nulling tomography with weak gravitational lensing*, *Phys. Rev. D* **72** (Aug., 2005) 043002–+, [[astro-ph/](#)].
- [86] R. B. Metcalf, *Gravitational lensing of high-redshift Type Ia supernovae: a probe of medium-scale structure*, *Mon. Not. R. Astron. Soc.* **305** (May, 1999) 746–754.
- [87] S. Dodelson and A. Vallenotto, *Learning from the scatter in type Ia supernovae*, *Phys. Rev. D* **74** (Sept., 2006) 063515–+, [[astro-ph/](#)].
- [88] A. R. Zentner and S. Bhattacharya, *Utilizing Type Ia Supernovae in a Large, Fast, Imaging Survey to Constrain Dark Energy*, *ArXiv e-prints* (Dec., 2008) [[arXiv:0812.0358](#)].
- [89] R. Stanek, D. Rudd, and A. E. Evrard, *The Effect of Gas Physics on the Halo Mass Function*, *ArXiv e-prints* (Sept., 2008) [[arXiv:0809.2805](#)].